Navigation Using Orthogonal Frequency Division Multiplexed Signals of Opportunity

THESIS

Jamie S. Velotta, Captain, USAF

AFIT/GE/ENG/07-31

DEPARTMENT OF THE AIR FORCE
AIR UNIVERSITY

AIR FORCE INSTITUTE OF TECHNOLOGY

Wright-Patterson Air Force Base, Ohio

AFIT/GE/ENG/07-31

Navigation Using Orthogonal Frequency Division Multiplexed Signals of Opportunity

THESIS

Presented to the Faculty

Department of Electrical and Computer Engineering

Graduate School of Engineering and Management

Air Force Institute of Technology

Air University

Air Education and Training Command

In Partial Fulfillment of the Requirements for the

Degree of Master of Science in Electrical Engineering

Jamie S. Velotta, B.S.E.E.

Captain, USAF

September 2007

AFIT/GE/ENG/07-31

Navigation Using Orthogonal Frequency Division Multiplexed Signals of Opportunity

Jamie S. Velotta, B.S.E.E.

Captain, USAF

Approved:

/signed/	13 September 2007
Dr. Richard K. Martin (Chairman)	date
/signed/	13 September 2007
Dr. John F. Raquet (Member)	date
/signed/	13 September 2007
Dr. Michael A. Temple (Member)	date

AFIT/GE/ENG/07-31

Abstract

The global positioning system (GPS) provides high-accuracy position measurements anywhere in the world. However, one limitation of this system is that a line-of-sight to multiple satellites is required; therefore, it is unsuitable to use indoors or in urban canyons. Also, in the presence of radio-frequency interference or jamming, GPS may be unavailable. Alternative methods of navigation and positioning are needed to either compliment GPS as a backup or for use in areas unreachable by satellites.

One alternative method of navigation that has been proposed is "Navigation via Signals of Opportunity (SoOP)." The SoOP navigation concept uses existing radio frequency signals that were not intended for navigation, and leverages knowledge of the transmitter locations to determine the receiver position.

Measurements that can be taken from SoOP include angle of arrival, signal strength (i.e., received power level), or time difference of arrival (TDOA) between multiple receivers. This research focuses on TDOA, since it is difficult to get high position accuracy from angle or power measurements. However, one difficultly encountered with using TDOA is that there must be either two transmitters sending the same signal or two physically separated receivers measuring the same transmission. Usually only one transmitter is available, hence a "reference receiver" must be placed at a known location, and the mobile receiver (whose position is to be determined) must cooperate with the reference receiver in some way. A second difficulty is that TDOA measurements generally require some form of correlation between the two received signals. This requires that the reference receiver retransmit much of its received signal to the mobile, using significant bandwidth. This work addresses how multicarrier modulation can alleviate these two difficulties.

Many broadcast multicarrier systems (e.g., terrestrial repeaters for satellite radio and European digital television) use multiple transmitters that transmit the same signal. This cannot be done with single carrier systems because it creates "multipath-like" environment at a receiver. However, due to their signal structure, multicarrier systems are very robust to the undesired effects of multipath. Ultimately, the result is that the reference receiver may no longer be needed for SoOP navigation.

Multicarrier systems also have the benefit of a well-defined signal structure in that the beginning and end of each symbol are identical. Thus, a receiver can identify block boundaries by searching for this repetition "blindly". In other words, the receivers do not require any prior knowledge of the transmitted signal. Thus, the mobile and reference receiver can independently locate block boundaries and calculate a variety of statistical features (i.e., mean, variance, etc.) of each symbol. The reference receiver then sends a sequence of symbol reception times and associated feature values to the mobile receiver, rather than retransmitting the entire signal. This leads to a significant reduction in backchannel bandwidth. This research demonstrates that this feature-based correlation technique can achieve accurate TDOA measurements for SNR values below 0 dB.

To my beautiful wife and children...

Acknowledgements

First and foremost, I want to give praise and thanksgiving to my Lord and Savior, Jesus Christ. He has blessed me with an abundant life even though I do not come close to deserving it. Without His grace, mercy, and love this entire process and Air Force experience would have been impossible for me to bear. *"Thank you for the strength to finish this lap in the race!"*

I also want to thank my wonderful wife. Her patience, passion, and tenderness have been such an inspiration to me. We have been through quite a lot together with two separate deployments inside of 12 months (of which I was gone for eight), the births of two gorgeous children, and moving everything we own in this world to four different states. I could not have asked for a better best friend to spend the rest of my life with. *"Thank you, and I love you."*

I would especially like to thank my thesis advisor, Dr. Martin. I don't think you realized what you were getting into when you agreed to be my advisor. I know that I definitely would not have finished my masters at all much less early without your guidance. I appreciate your unwavering patience with me. I also wish to thank my committee members, Dr. Temple and Dr. Raquet. Your guidance and expertise were crucial to the completion of this research.

Finally, I thank the Air Force for allowing me the great opportunity to serve my country. I am very proud for the experiences afforded to me. I pray that my efforts will allow me to leave the Air Force in better condition than when I entered it.

Jamie S. Velotta

Table of Contents

List of Figures

List of Tables

List of Abbreviations

Abbreviation		Page
OFDM	Orthogonal Frequency Division Multiplex	1
SOI	Signal(s) of Interest	1
RF	Radio-Frequency	1
INS	Inertial Navigation System	1
SoOP	Signal(s) of Opportunity	2
AM	Amplitude Modulated	2
FM	Frequency Modulated	2
DVB	Digital Video Broadcast	2
DAB	Digital Audio Broadcast	2
CDMA	Code Division Multiple Access	2
TDOA	Time-Difference-Of-Arrival	3
AWGN	Additive White Gaussian Noise	3
LORAN	LOng RAnge Navigation	6
LF	Low Frequency	6
LOP	Line of Position	6
TOA	Time of Arrival	7
AOA	Angle of Arrival	7
WMAN(s)	Wireless Metropolitan Area Network(s)	9
WLAN(s)	Wireless Local Area Network(s)	9
WPAN(s)	Wireless Personal Area Network(s)	9
IEEE	Institute of Electrical and Electronics Engineers	9
MIMO	Multiple-Input Multiple-Output	9
WiMax	Worldwide Interoperability for Microwave Access	9
LAN	Local Area Network(s)	10

Abbreviation		Page
MAN	Metropolitan Area Network(s)	10
OFDMA	Orthogonal Frequency Division Multiple Access	10
ETSI	European Telecommunications Standards Institute	10
FDMA	Frequency Division Multiple Access	12
ISI	Inter Symbol Interference	14
QAM	Quadrature Amplitude Modulation	15
PSK	Phase-Shift Keying	15
QPSK	Quadrature Phase-Shift Keying	17
BPSK	Binary Phase-Shift Keying	17
FFTs	Fast Fourier Transforms	18
IFFTs	Inverse Fast Fourier Transforms	18
ICI	Inter Channel Interference	19
LOS	Line-of-Sight	20
SNR	Signal-to-Noise Ratio	25

Navigation Using Orthogonal Frequency Division Multiplexed Signals of Opportunity

I. Introduction

This chapter provides the necessary motivation for researching the navigation potential of multicarrier signals, specifically orthogonal frequency division multiplexed (OFDM) signals, to include background, research goals, and assumptions made in order to limit the scope of research. Additionally, a review of related research is briefly made followed by a justification for using OFDM signals as the choice signals of interest (SOI). This chapter is then concluded with an organizational outline of the remaining chapters.

1.1 Background

Currently, GPS is the most widely used system in the world for precision navigation and timing; however, there are certain circumstances where GPS may be degraded or unavailable. One such instance may be in urban environments, inside buildings, or any location where acquisition of multiple satellites is not possible. Another example of possible GPS unavailability is in the presence of intentional (i.e. jamming) or unintentional radio-frequency (RF) interference. Finally, since GPS is a single system, a single unexpected failure could render the entire system inoperable. There are other systems that can provide accurate short-term navigation solutions, but they are unable to provide unconditional position capabilities. One such system is an inertial navigation system (INS) [11]. Therefore, additional systems must be developed to guarantee "GPS quality" navigation capabilities under any given circumstance.

Precision Engagement, according to the Joint Vision 2010, is defined as the capability "that enables our forces to locate the objective or target, provide responsive command and control, generated the desired effect, assess our level of success, and retain the flexibility to re-engage with precision when required" [1]. In order for the Air Force to establish and maintain this core competency during operations it is imperative that non-GPS technologies be employed where GPS may currently fail or be denied. One such category of navigation potential utilizes Signals of Opportunity (SoOP). SoOP are defined as any RF signals which are not specifically designed for navigational purposes. Three examples of SoOP include broadcast single carrier systems (i.e. analog television broadcasts, Amplitude Modulated (AM) and Frequency Modulated (FM) radio signals), cellular communications, and broadcast multicarrier systems (i.e., terrestrial repeaters for satellite radio, European Digital Video Broadcast (DVB) and Digital Audio Broadcast (DAB), and wireless networking standards such as 802.11a) [11], [14], [17], [22]. Each of the aforementioned SoOP have specific signal properties and characteristics which could be exploited for navigation purposes.

The navigation potential of broadcast single carrier systems, such as AM, FM, and analog television radio signals, have been previously investigated in [11] and [14]. Both [11] and [14] found promising results for using these signals for navigational purposes. Since broadcast single carrier systems typically transmit one thousand to one million times more power than GPS signals (depending on the system) they proved in certain circumstances better suited for indoor and urban environment navigation [11], [14]. However, single carrier systems are heavily affected by multipath (see Section 2.2).

Cellular communication waveforms, such as the ones used for the Code Division Multiple Access (CDMA) IS-95 Digital Cellular Network, hold distinct properties that make them potential nominees for navigational use. One specific characteristic is that the IS-95 Digital Cellular Network utilizes a pilot channel for user-to-system synchro-

nization. This pilot channel transmits a 32,767 bit pseudo-random "short" code that repeats 37.5 times per second. Since the pseudo-random bit pattern and modulation scheme are both known, it is possible to use correlation techniques to estimate the signal's reception time. With the reception time of four or more independent signals, position estimations can then be calculated. Since the IS-95 Digital Cellular Network depends on GPS for time synchronization, it is unfortunately a poor candidate for navigation when GPS is unavailable [11].

Multicarrier systems, such as DVB, DAB, and 802.11a/n, have many advantages that make them ideal navigation SoOP candidates [22]. In many broadcast multicarrier systems, multiple transmitters each transmit the same signal. This cannot be done within single carrier systems because it creates multipath (See Section 2.2) in the received signal. However, multicarrier systems are very robust to multipath which may potentially result in no longer needing a dedicated reference receiver for position calculations. Additionally, multicarrier systems also have a well-defined, repetitive signal structure. With a repetitive signal structure it is possible for two independent receivers to calculate specific signal characteristics and correlate the findings in order to generate accurate position estimates.

1.2 Research Goals

The primary goal of this research is to prove the concept that OFDM signals (i.e., multicarrier signals) are indeed good candidates to use in time-difference-of-arrival (TDOA) navigation systems. Performance is studied by analyzing the effects of Additive White Gaussian Noise (AWGN) on two receivers' (a reference and mobile receiver) ability to correctly estimate the time difference of signal reception.

The secondary goal of this research is to reduce the back channel bandwidth (i.e., amount of data transferred) between the reference receiver and the mobile receiver. Typically, both the reference receiver and mobile receiver obtain the transmitted

signal with two different channel realizations. The reference receiver then transfers a section/window of the received signal to the mobile receiver. Once received at the target receiver, it correlates the two signals to determine the reception time difference and ultimately TDOA. In this research, the two receivers independently calculate block boundaries and then calculate statistical "features" of every block. Using this method, the mobile receiver only needs to compare "features" and symbol boundaries and not the entire received reference signal, thus reducing overall bandwidth between the two receivers. Performance is evaluated by analyzing the effects of varying the number of block features (i.e., the window size) sent to the target receiver.

1.3 Assumptions

For this research, the following assumptions were made about SoOP and the receiver capabilities:

1. SoOP have an established infrastructure in and around the Area of Responsibility
2. SoOP operate within frequency range of the receivers
3. SoOP have known modulation format and signal structure (OFDM for this research)
4. Transmitter location is known
5. No multipath at receivers
6. No frequency offset/phase noise between the receivers and transmitter

For successful navigation in a GPS denied environment, three of the aforementioned assumptions focus on the SoOP. First, the SoOP must be readily accessible. Therefore, a preestablished SoOP infrastructure is necessary. Next, for this research it is assumed that a receiver can be built to collect the SOI. In the case of this thesis, the SOI has a known modulation format of OFDM with defined, constant data and

cyclic prefix lengths. Finally, all SoOP transmitter locations are known. For some civilian infrastructures, such as the terrestrial repeaters for satellite radio, a simple web query can produce maps and geolocations of all operational transmitters. This information is also available from the Federal Communication Commission or foreign government equivalent.

Two additional assumptions were made which pertain specifically to the receivers. Most real-world receivers are affected by the phenomenon of multipath, but for this proof-of-concept, it is assumed that there is no multipath present. This assumption was implemented to limit the scope of this thesis.

The final assumption states that there is no frequency offset or phase noise caused by oscillator inaccuracies. OFDM is very sensitive to these frequency effects between the receiver and transmitter [16], [20], [23]. This assumption was made due to the research time constraints.

1.4 Related Research

This section discusses multiple navigation systems, both TDOA and non-TDOA based, that have been researched and presented to the navigation community. The first part of this section covers navigation systems which use TDOA followed by the non-TDOA navigation systems.

1.4.1 TDOA-based Navigation Systems. These systems focus on measuring the *difference* in arrival times of two transmitted signals by a single receiver, or by differencing the arrival time of a single signal at two separate receivers. For this thesis, the latter definition of TDOA was implemented. One of the two receivers, known as the target or mobile receiver, has an unknown location while the other receiver, referred to as the reference receiver, has a known location. These two receivers have a data link between them, where the reference receiver shares signal reception information with the target receiver. The difference in the reception time between the

two receivers allows for a position calculation (See Figure 1.1). Two systems that use TDOA techniques for navigation are the LOng RAnge Navigation (LORAN) and the NAVSYS Corporation's GPS Jammer and Interference Location System.

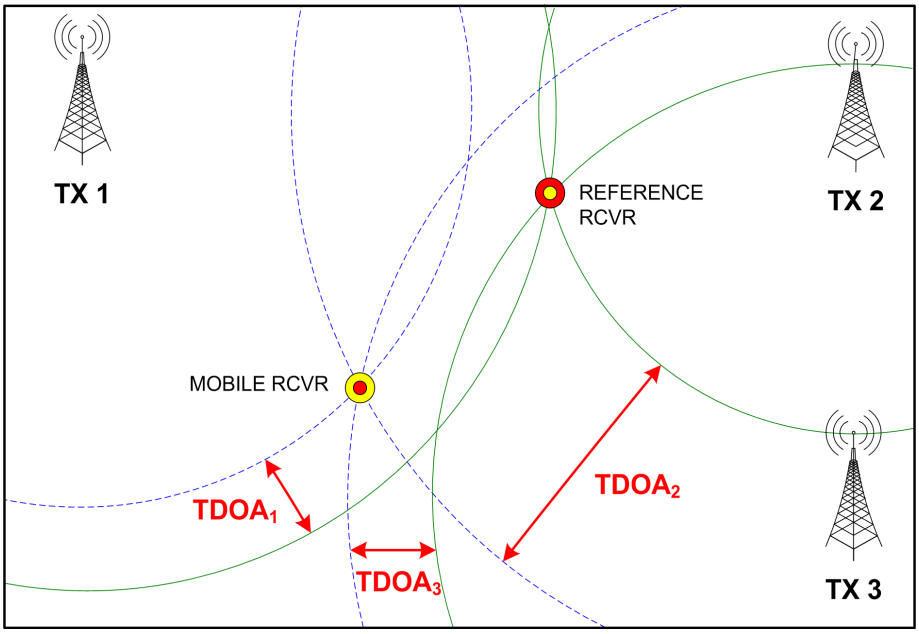

Figure 1.1: TDOA Technique. Position is calculated by differencing the arrival time of a single transmission signal received at two separate receivers.

LORAN. LOng RAnge Navigation operates in the Low Frequency (LF) band at 90 to 110 kHz. In this terrestrial system, multiple synchronized transmitters radiate pulses of RF energy. An airborne or shipborne receiver measures the TDOA of the pulses from the different transmitters. Each measured TDOA defines a hyperbolic line of position (LOP) for the receiver. The intersection multiple LOPs give the user an accurate navigation solution [18].

GPS Jammer and Interference Location System. NAVSYS corporation designed a navigation system which lessens the effects of GPS jamming and/or interference. The system uses multiple terrestrial receivers at known locations to determine the position of a single transmission source (i.e. the GPS jamming device).

Once the GPS interference source's location is known it then can be mitigated or avoided [11].

1.4.2 Non-TDOA-based Navigation Systems. Three additional position estimation methods for calculating the location of a target receiver are as follows:

- Signal Strength Measurement
- Time of Arrival (TOA)
- Angle of Arrival (AOA)

Signal Strength Measurement. This method of radiolocation uses a known mathematical model that depicts the path loss attenuation over distance between a mobile receiver and a transmitter. By detecting multiple transmitters, the mobile receiver's location can be calculated more accurately; however, this measurement of signal strength is susceptible to error mainly due to multipath [9].

Time of Arrival. In TOA calculations, the distance between a mobile receiver and a transmitter is measured by finding the one-way propagation time between the two. This measurement then provides a geometric circle, centered on the transmitter, on which the mobile receiver must lie. Similar to signal strength measurements, receiving signals from more than one transmitter can resolve ambiguities because the mobile receiver will lie on the intersection of the circles [9]. Figure 1.2 illustrates this intersection.

TOA calculations require all transmitters be time synchronized. If all of the transmitters are synchronized, then synchronizing the receiver is unnecessary because the receiver clock error is constant for all transmitters. This clock error can then be accounted for with additional calculations; thus eliminating the receiver clock error altogether from the TOA measurements [9].

Angle of Arrival. When using the AOA technique, a mobile receiver estimates the signal reception angles for two or more sources with known locations. It

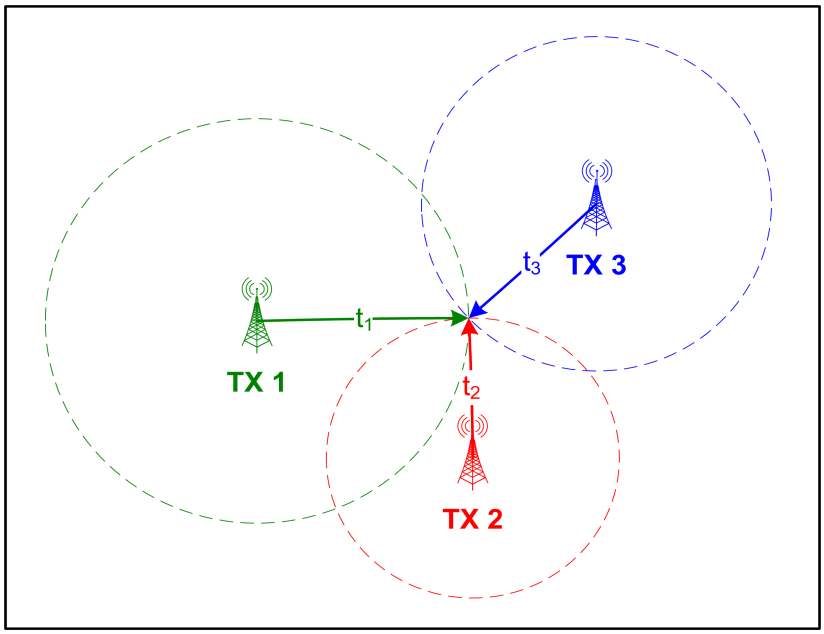

Figure 1.2: TOA Technique. Position is found by determining the one-way propagation time between multiple transmitters and the mobile receiver.

does this by comparing either the carrier-phase or signal amplitude across multiple antennas. From these calculations, the target receiver's position is triangulated by the intersection of the angle line from each signal source. Figure 1.3 illustrates the improvement in accuracy when using more than two sources. This passive navigation method is easily implemented. However, AOA calculations are very susceptible to range. As the distance from the source increases, the position accuracy decreases [9].

1.5 Justification

Over the past decade, the world of wireless communications has taken off. Multicarrier transmission systems, more specifically OFDM systems, have become the digital communication modulation/multiplexing scheme of choice for many wireless environments. This modulation preference has sparked the development and construction of multiple OFDM wireless infrastructures in many locations where GPS may be unavailable. With the importance of precision navigation for first responders,

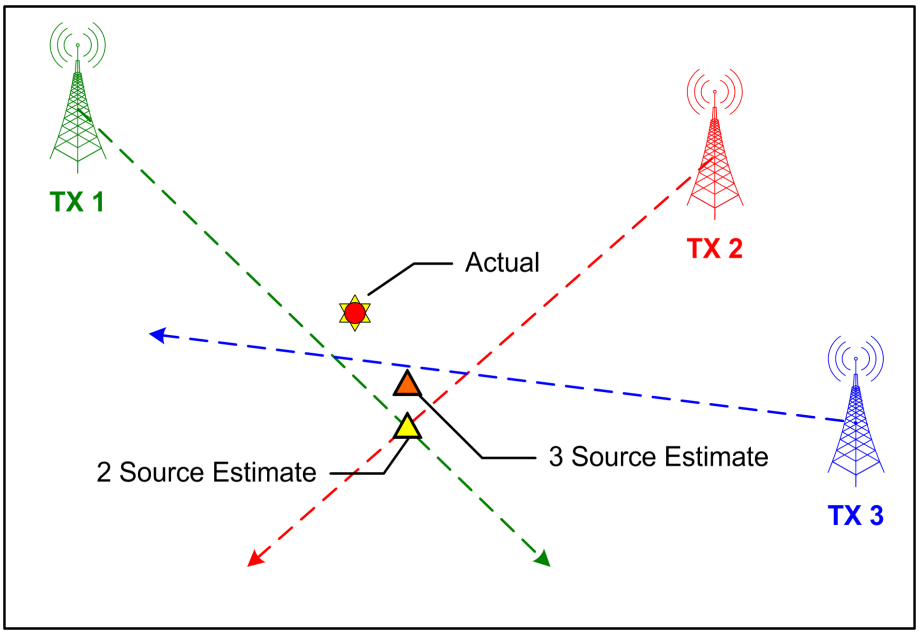

Figure 1.3: AOA Technique. Position is calculated by determining the intersection of the angle line from each transmitter.

emergency services, and military operations it is essential that OFDM be studied for its navigation potential.

Some communication technologies which implement OFDM are listed below [22]. Following the list is a brief description of Wireless Metropolitan Area Networks (WMAN(s)), Wireless Local Area Networks (WLAN(s)), and Wireless Personal Area Network (WPAN(s)).

- Institute of Electrical and Electronics Engineers (IEEE) standards
  - 802.11 a/g, WLAN
  - 802.11n, WLAN, Multiple-Input Multiple-Output (MIMO) OFDM
  - 802.15.3 a, WPAN
  - 802.16 a, Worldwide Interoperability for Microwave Access (WiMax), WMAN

  - 802.22, Local Area Networks (LAN), Metropolitan Area Network (MAN), Orthogonal Frequency Division Multiple Access (OFDMA)
- European Telecommunications Standards Institute (ETSI) standards
  - DAB terrestrial repeaters, Digital Radio
  - DVB terrestrial repeaters, High-Definition Television
- Satellite Radio (Terrestrial Repeaters)
  - XM and SIRIUS terrestrial repeaters

WPANs, WLANs, and WMANs are all terms used to describe different area networks that support wireless transmissions between systems. However, some of the primary differences between the three networks are coverage area, power requirements, and data rates. WPANs are used to transmit data over moderately short distances ($\leq$ 10 meters) between few systems, typically require no infrastructure, and consume minimal power at low data rates [2]. WLANs, on the other hand, usually have higher data rates and a larger coverage area (between 10 and 250 meters). To accommodate this increased coverage area, systems apart of or utilizing a WLAN have higher power requirements than systems on WPANs [3]. WLANs typically have an in place infrastructure. Finally, WMANs' coverage area is usually measured in kilometers, and these networks support much higher data rates to end systems.

1.6 Organizational Outline

Chapter II provides a detailed description of the OFDM signaling structure and TDOA fundamental algorithms. *Chapter III* explains the methodology used in symbol detection, feature, and TDOA calculations. *Chapter IV* details the results from the simulations described in *Chapter III*. Finally, *Chapter V* gives an overall summary and conclusions of the thesis along with potential follow-on areas of study.

II. Technical Background

This chapter provides the technical background necessary for understanding the overall concepts of this research. First, an in-depth description of OFDM signaling is given followed by a brief discussion on the phenomenon of multipath and its effects on RF signals. Finally, a TDOA algorithm with respect to the OFDM signal structure is derived.

2.1 OFDM Signals

OFDM is a communication method which can be viewed as a modulation scheme or a multiplexing technique. In OFDM, the carrier spacing is selected such that each subcarrier is orthogonal to the other subcarriers. Two signals are spectrally orthogonal if the following condition is true:

$$\int_0^{n \cdot T} \chi_1(f) \cdot \chi_2^*(f) \cdot df = 0, \quad n = 1, 2, 3, ... \tag{2.1}$$

where T is the period, χ_1 and χ_2 are input signals, and $*$ denotes complex conjugate.

Figure 2.1 depicts the overall system design of a typical OFDM system. The transmitter consists of an encoder, interleaver, "constellation mapper", OFDM multiplexer, and RF transmitter, while the receiver is made up of a RF receiver, synchronization mechanism, OFDM demultiplexer, "constellation demapper", de-interleaver, and decoder.

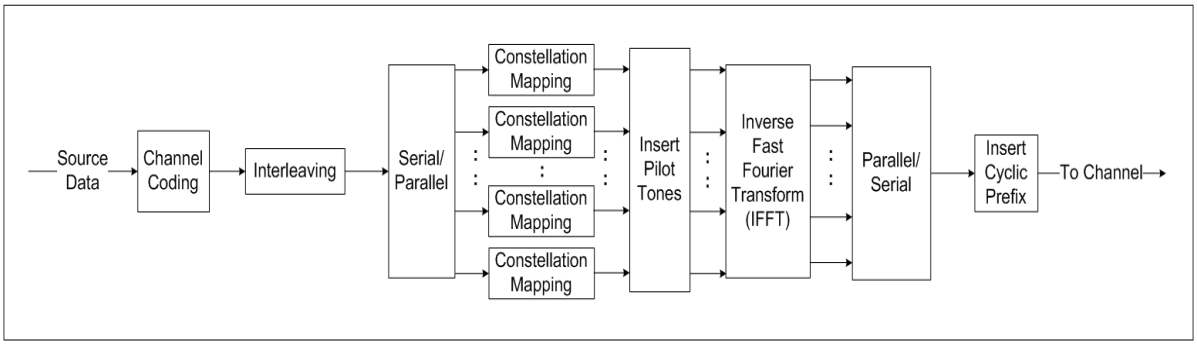

(a) OFDM Transmitter

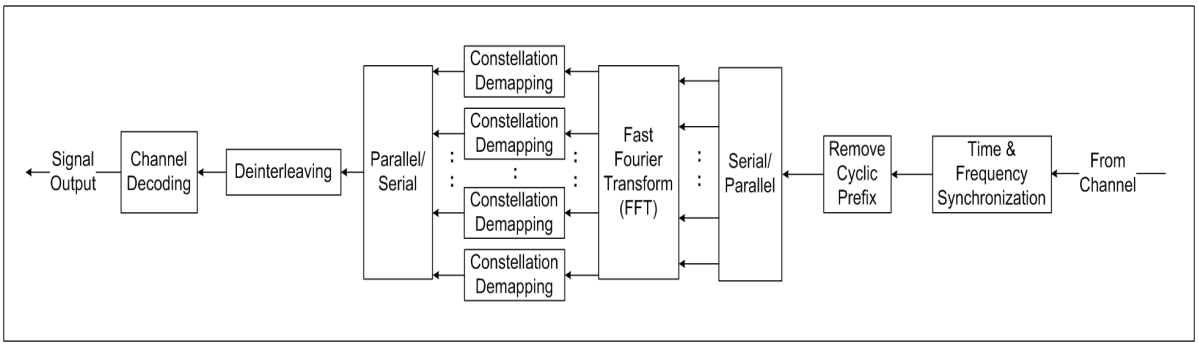

(b) OFDM Receiver

Figure 2.1: Block Diagram of OFDM Communication System [19].

OFDM is a special case of a Frequency Division Multiple Access (FDMA) system. In FDMA, users access a communication channel simultaneously, but they all utilize different parts of the spectrum. Since there is physical frequency separation between the adjacent subcarriers, the interference between these adjacent channels is avoided. The frequency separation between adjacent subcarriers is known as the guard band. However, in an OFDM system, the subcarriers have overlap, but since the subcarriers are orthogonal per (2.1), there is no adjacent channel interference. Because of this spectral overlap, OFDM is much more bandwidth efficient when compared to a FDMA system with the same number of channels [10]. Figure 2.2 gives a graphical comparison of a FDMA system and an OFDM system in the frequency domain.

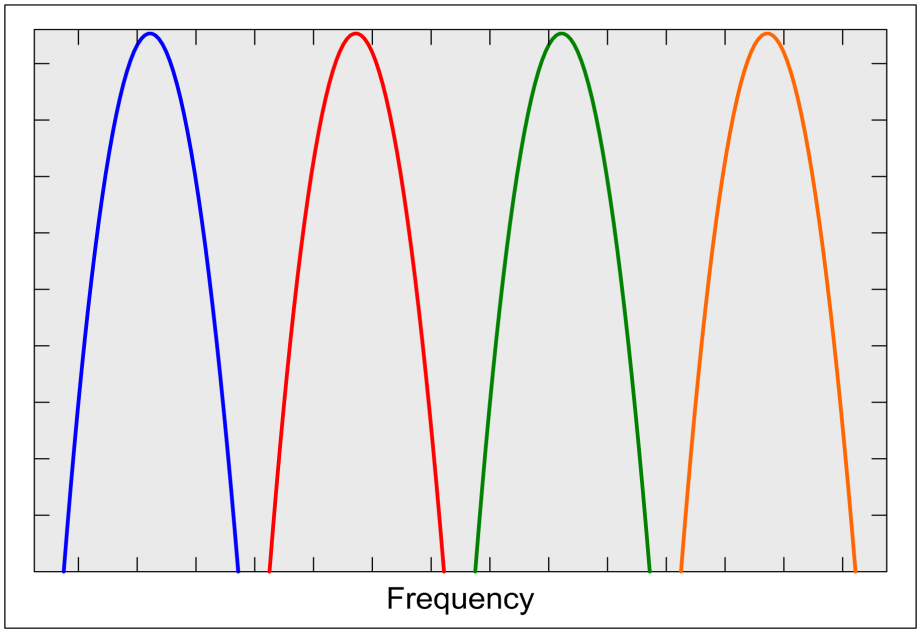

(a) FDMA (Frequency Domain)

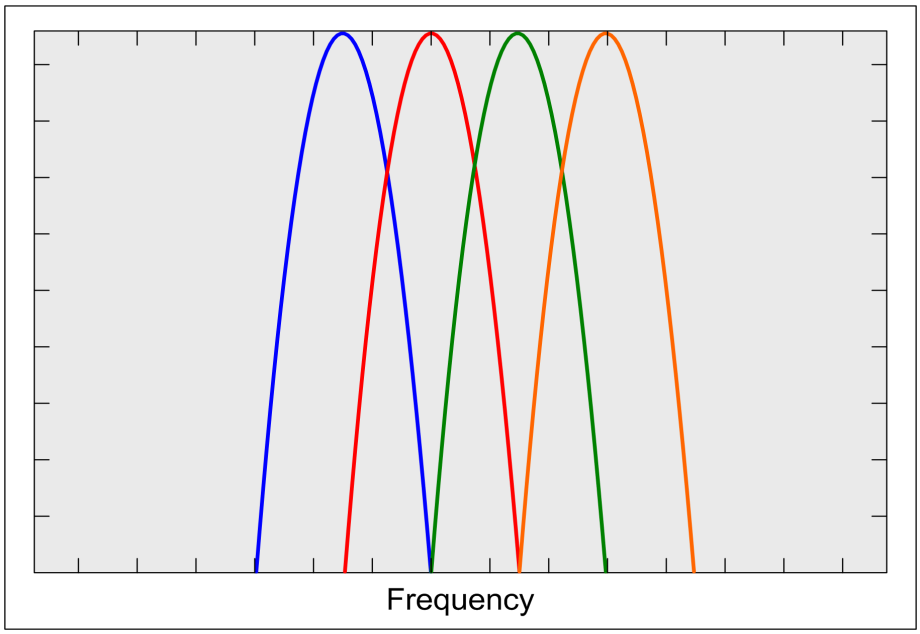

(b) OFDM (Frequency Domain)

Figure 2.2: FDMA vs. OFDM. (a) Four FDMA channels with frequency guard bands. (b) Four OFDM orthogonal channels.

Table 2.1: IEEE Std 802.11a Rate Dependent Convolutional Rates [3].

Data Rate (Mbits/s)	**Modulation**	**Coding Rate**
6	BPSK	1/2
9	BPSK	3/4
12	QPSK	1/2
18	QPSK	3/4
24	16-QAM	1/2
36	16-QAM	3/4
48	64-QAM	2/3
54	64-QAM	3/4

2.1.1 Coding. Channel coding is implemented to prevent the effects of inter symbol interference (ISI). ISI is a distortion that occurs when a previously transmitted symbol interferes with the symbol currently being received. Convolutional, block, and Reed-Solomon coding along with Trellis coded modulation are all coding methods that have been recommended for OFDM systems in order to combat ISI [15], [24]. Table 2.1 shows the convolution coding rates for the IEEE standard 802.11a. In many cases, multiple types of encoding are performed on a signal at different stages in an OFDM transmitter to improve coding gain at a relatively small implementation cost [19]. For example, in 802.16a the signal uses both Reed-Solomon and pragmatic Trellis Coded modulation before being mapped to a specific modulation constellation [4].

2.1.2 Interleaving. In many digital communication systems, decoders are used to classify codewords from a string of message bits even when some bits contain errors. In other words, a channel decoder is built to correctly fix up to a specific number of bits within a message. If the decoder's bit error threshold for a given message is exceeded then the correct codeword cannot be decoded. The purpose of interleaving is to prevent a string or burst of simultaneous bit errors to enable the decoder to correctly identify the codeword. Figure 2.3 shows the typical functionality of a block interleaver/de-interleaver.

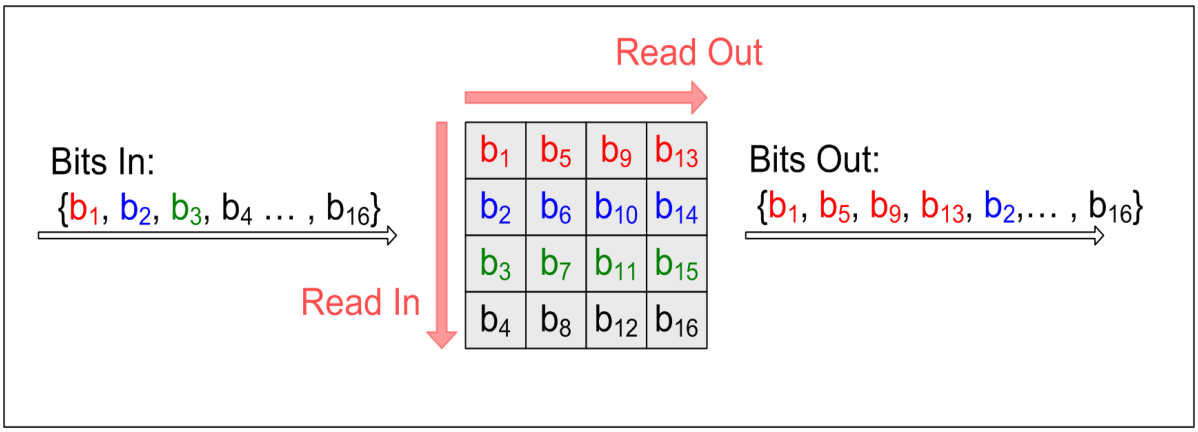

(a) Interleaver

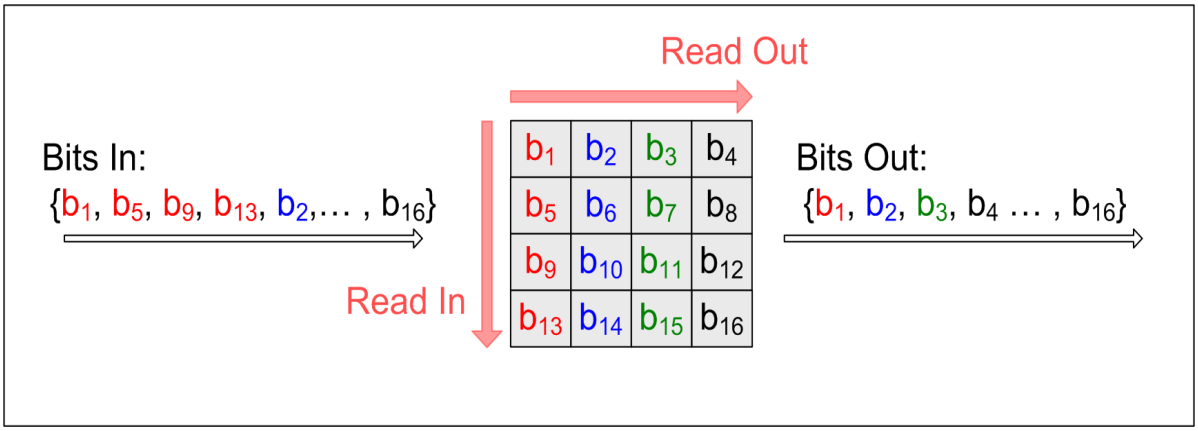

(b) De-Interleaver

Figure 2.3: Block Interleaving Process. (a) Interleaver. (b) De-Interleaver.

! This thesis does not use the encoding/decoding or interleaving/de-interleaving processes since a random number generator was used to create the input signal to the OFDM system. The statical properties of the simulated signal are the same as if the aforementioned processes were implemented on a given signal.

2.1.3 Constellation Mapping. Bits are demultiplexed into N parallel data streams, where N is the symbol length. Following through Figure 2.1, the N bit streams are then mapped to some modulation constellation, possibly quadrature amplitude modulation (QAM) or phase-shift keying (PSK). Figure 2.4 shows constella-

tion diagrams for different modulation schemes. For this research, the N data streams were mapped to a 64-QAM constellation.

M-ary QAM is a hybrid modulation technique which has amplitude and phase modulation. Each c^{th} signal is represented by [6]:

$$x_c(t) = \sqrt{\frac{2 \cdot E_0}{T}} \cdot x_I(t) \cdot \cos\left[(2\pi) \cdot f_c \cdot t\right] + \sqrt{\frac{2 \cdot E_0}{T}} \cdot x_Q(t) \cdot \sin\left[(2\pi) \cdot f_c \cdot t\right], \quad iT \leq t \leq (i+1)T \tag{2.2}$$

where $x_c(t)$ is the complex baseband signal, $x_Z(t) = x_I(t) + j \cdot x_Q(t)$, converted to a passband signal. $x_I(t)$ and $x_Q(t)$ represent the "in phase" and "quadrature" portions of the complex signal, respectively.

2.1.4 Pilot Tones. OFDM symbols are comprised of data and pilot tones (NOTE: "Tone(s)" and "frequency(ies)" may be used interchangeably throughout the duration of this thesis). The pilot tones are known by the system receiver and used primarily for frequency synchronization. For 802.11a, the pilot tones are a pseudo random sequence of ± 1's [3]. Pilot tones can be inserted in any sequence/constellation with respect to the signal's time vs. frequency structure. Figure 2.5 illustrates the pilot tone constellation for ESTI's DVB standard [5]. For this research, an arbitrary pilot tone constellation was chosen merely to confirm symbol estimations made by the overall feature correlation process. However, the feature-based symbol estimation method discussed in Chapter III is a non-cooperative scheme implemented with no need for pilot tone knowledge. Additionally, pilot tones were not even considered for the proposed feature-based estimation process. In any case, Figure 2.6 depicts the pilot tone constellation used for the simulations in this research.

2.1.5 OFDM Modulation via Inverse Fast Fourier Transforms. Historically, it has been extremely difficult to implement OFDM in high-speed digital communications due the complex computations involved with multicarrier modulation/demod-

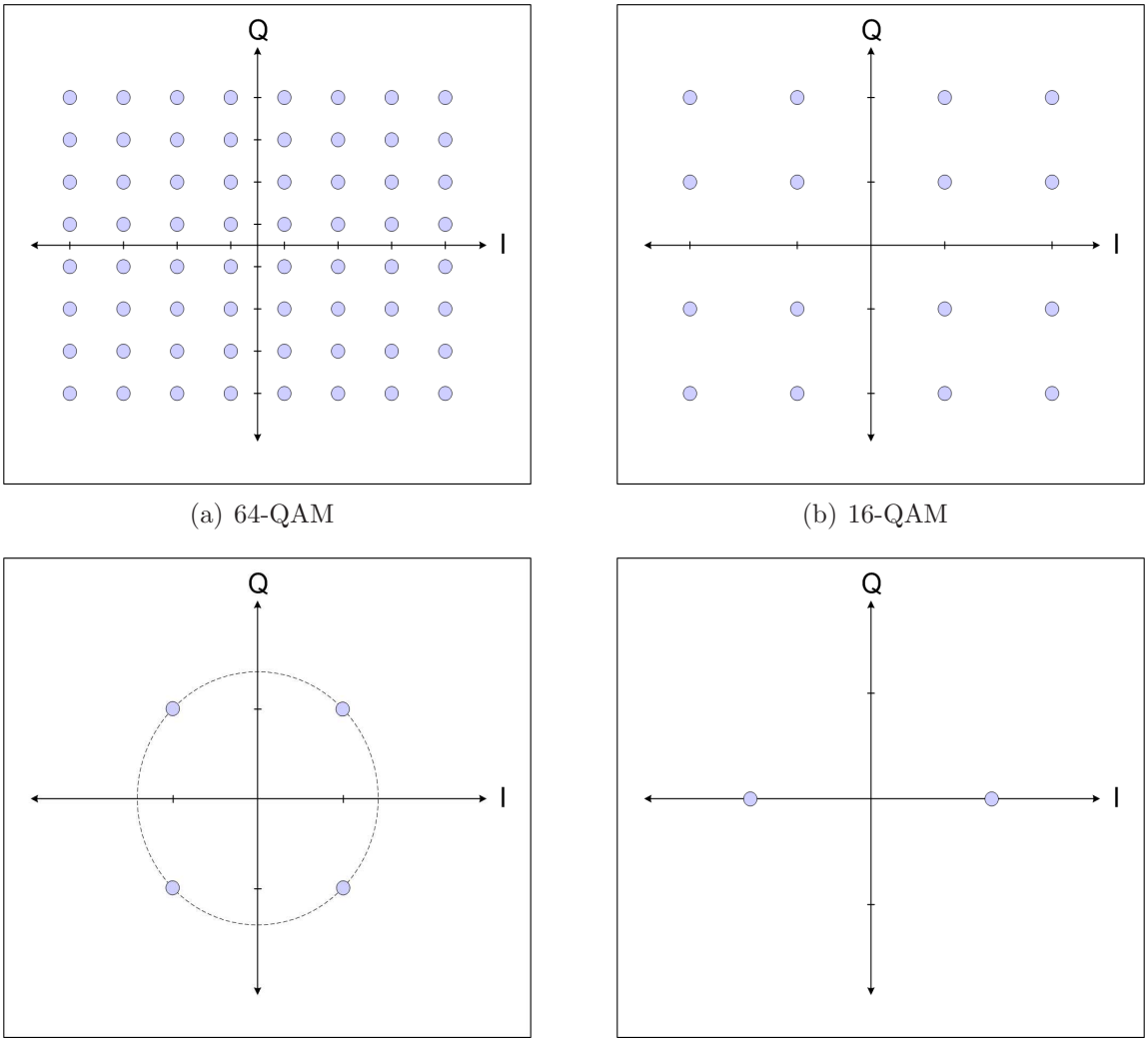

(a) 64-QAM

(b) 16-QAM

(c) 4-QAM / QPSK

(d) BPSK

Figure 2.4: QAM/PSK Constellations. (a) 64-QAM. (b) 16-QAM. (c) 4-QAM/Quadrature Phase-Shift Keying (QPSK) (d) Binary Phase-Shift Keying (BPSK)

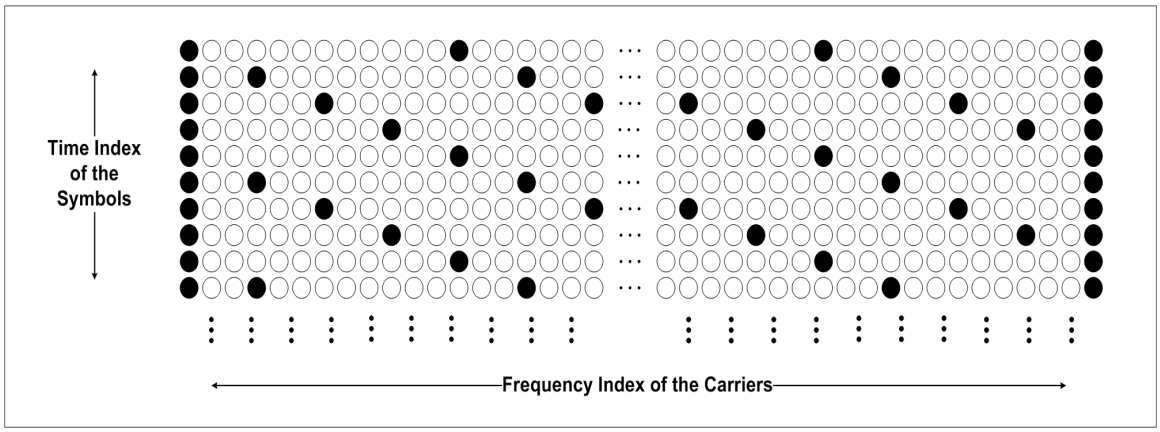

Figure 2.5: DVB Pilot Tone Constellation [5].

ulation. However, the advances in digital signal processing in the 1980's and 1990's have made OFDM implementation less computationally intense and thus more cost effective. More specifically, the use of Fast Fourier Transforms (FFTs)/Inverse Fast Fourier Transforms (IFFTs) eliminated the need for arrays of sinusoidal generators and coherent demodulation, all of which are required for parallel communications.

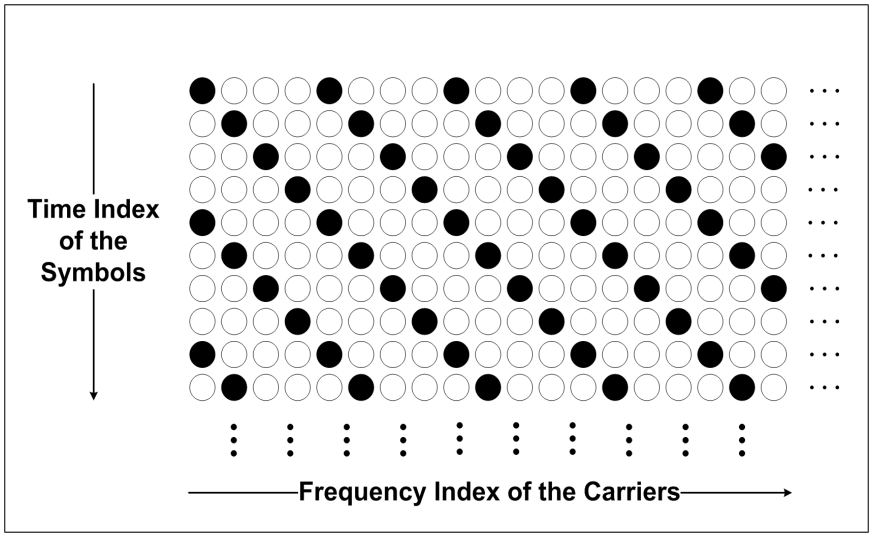

Figure 2.6: Pilot Tone Constellation Used for Research. The length of Frequency Index of the Carriers is 64 carriers. The length of the Time Index of the Symbols is 64 symbols. The constellation repeats every 64 symbols.

From Figure 2.1, IFFTs are used to modulate a block of encoded/mapped data; while FFTs are used for demodulation. Since the purpose of this thesis is not to decipher (i.e., demodulate/decode) the transmitted signal for communication purposes, the remaining focus of this section is on the modulation technique (i.e., the IFFT) in the OFDM transmitter. The following shows the equations needed for calculating the IFFT.

$$x_k(n) = \frac{1}{N} \cdot \sum_{k=0}^{N-1} S_n(k) \cdot W_N^{-k \cdot n}, n = 0, 1, ..., N-1 \tag{2.3}$$

where

$$W_N = e^{-\frac{j \cdot (2\pi)}{N}} \tag{2.4}$$

is known as the "twiddle factor" [13]. $S_n(k)$ represents the n^{th} data symbol at the k^{th} sample. These variables, n and k, range from 0 to $N-1$ where N is the total number of samples and ultimately the length of the IFFT. Note that the input signal,$S_n(k)$, is complex, (i.e., $S_n(k) = a_n(k) + j \cdot b_n(k)$), for this research.

2.1.6 Cyclic Prefix. The time domain OFDM signal is cyclically extended to mitigate the effects of ISI and interchannel interference (ICI). This is accomplished by replicating the last ν samples of the OFDM symbol and concatenating them to front of the symbol, thus creating a guard period between symbols. In practice, this guard period needs to exceed the maximum expected delay spread of the channel to avoid ISI and/or ICI. In other words, as long as the maximum excess delay, τ_{max}, is less than the cyclic prefix length, T_g secs (or ν samples), the distorted signal remains within the cyclic prefix interval and be removed by the receiver, thus eliminating ISI and/or ICI [12].

Figure 2.7 graphically illustrates how the cyclic prefix is appended to the beginning of the symbol inside the signal structure before transmission. This results in transmitting a symbol that is now $N + \nu$ samples (or $T + T_g$ seconds) long.

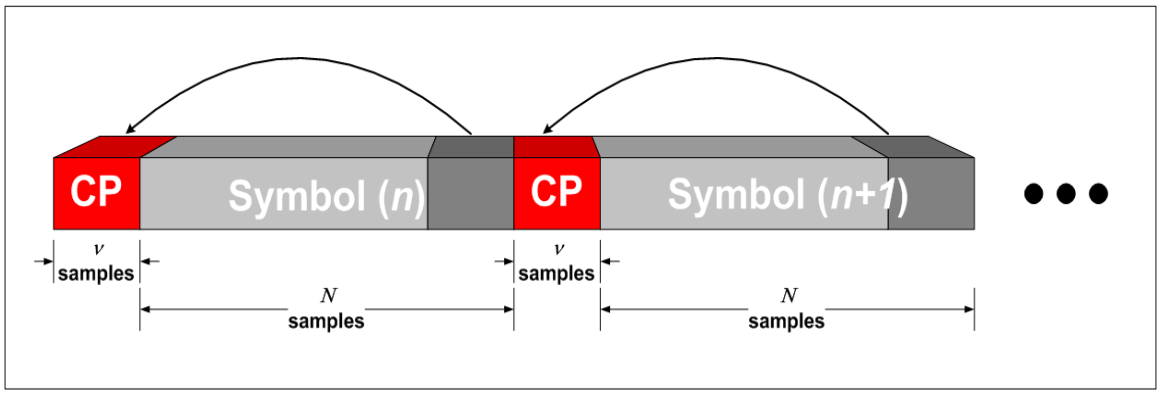

Figure 2.7: Cyclic Prefix Extension. The last ν samples are appended to the beginning of the symbol to create the guard interval between symbols.

Mathematically, the cyclic prefix's purpose is to convert the linear convolution of the transmitted signal with the channel to a circular convolution and thereby causing the FFT of the circularly convolved signal and channel to simply be the product of their respective FFTs.

2.2 Multipath

Multipath is a propagation phenomenon where a RF signal reaches a receiver by more than one path. It can be caused by atmospheric reflection and/or refraction and also from terrestrial reflection from objects such as buildings, mountains, etc. Figure 2.8 illustrates how multipath at a receiver may occur. All received signals other than the line-of-sight (LOS) signal are classified as multipath. The LOS signal is typically the most dominant of all other received signals since the other signals take longer to reach the receiver. However, an exception to the dominant LOS case occurs when the LOS signal is obstructed and a reflected signal then becomes dominant. Multipath signals combine and/or distort the dominant signal in either a constructive or destructive manner by adding signals with different attenuation, time-delays, and phase shifts [7]. The distortion amount depends on a number of different factors such

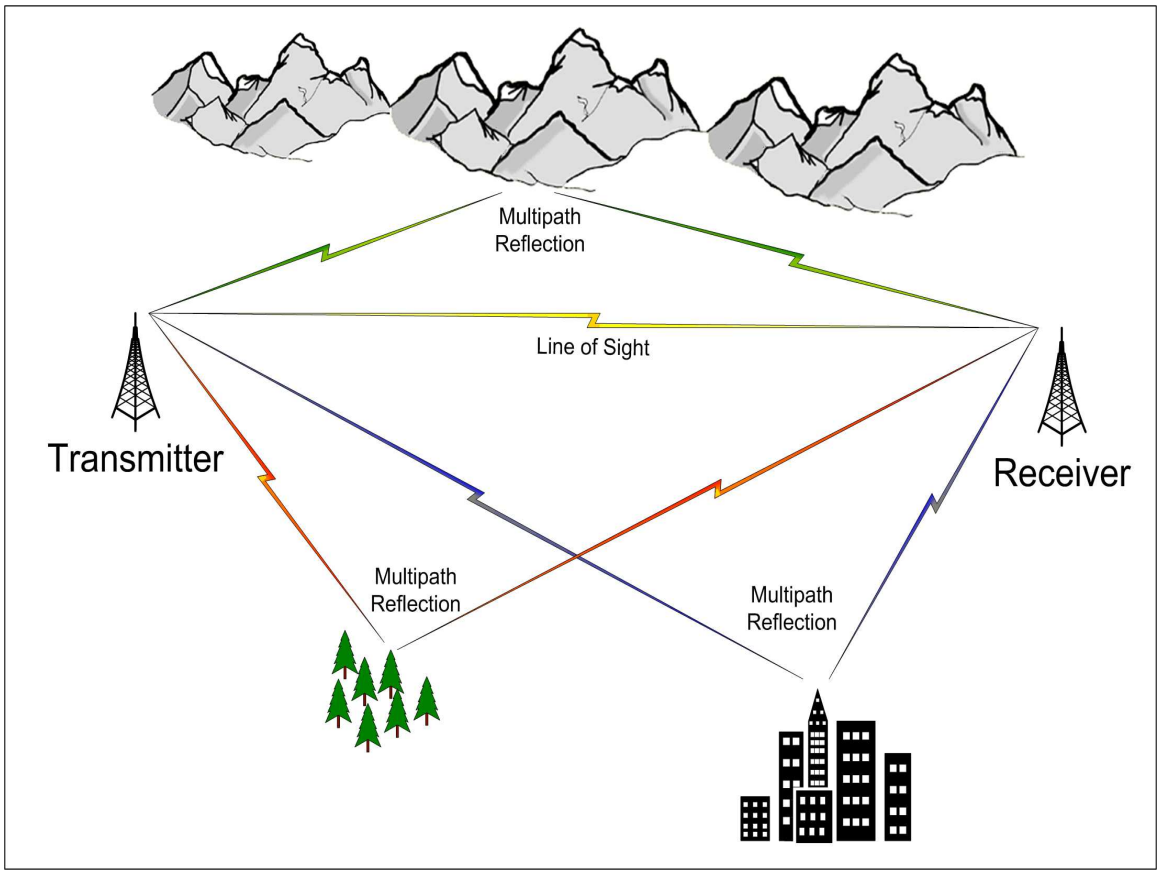

Figure 2.8: Multipath. The receiver received multiple signals of the same transmission due to multipath.

as relevant power of any dominant signal and range in the delays experienced by the multipath signals [8].

! This thesis does not consider the effects of multipath. This research was simulated under the assumption that the receivers (reference and mobile) only receive one dominant LOS signal.

III. Methodology

This chapter describes the methodology used for performing the proof of concept simulations for determining individual OFDM symbol boundaries, symbol features, and symbol reception time difference between the reference and mobile receivers. Ultimately, these calculations provide a TDOA estimate of the mobile receiver. Section 3.1 provides an overview of the simulated system, Sections 3.1.2 and 3.1.3 detail the processes necessary for determining symbol differences between receivers, and Section 3.2 explains the TDOA estimation process.

3.1 Model Overview

The model used in this research is depicted in Figure 3.1. It consist of one OFDM transmitter and two receivers, a reference and mobile. The transmitter in this model is the same as described in Chapter 2. The transmitter sends an OFDM signal over two different AWGN channels to the two receivers, i.e, each receiver receives a different noise realization of the transmitted signal. Figure 3.2 depicts the block diagram of both the reference and mobile receivers. Recall from Section 2.2 that it is assumed there is no multipath interference in this model.

3.1.1 Symbol Boundary Correlator. From Figure 3.2, the first process that both receivers perform on the received signal is determine the symbol boundaries. Recall from Section 2.1.6, that a total transmitted OFDM symbol is comprised of N data samples plus the cyclic prefix, which is ν samples long. Therefore, one complete transmitted symbol is $N+\nu$ (64+16 = 80 for simulations) samples long. Knowing that the transmitted signal follows this symbol structure for every symbol, it is possible to calculate the symbol boundaries using the following equation to correlate the cyclic prefix with the end of the symbol [21]:

$$R_{rx}(m) = \sum_{k=m}^{m+\nu-1} y_{rx}(k) \cdot y_{rx}^{*}(k+N) \tag{3.1}$$

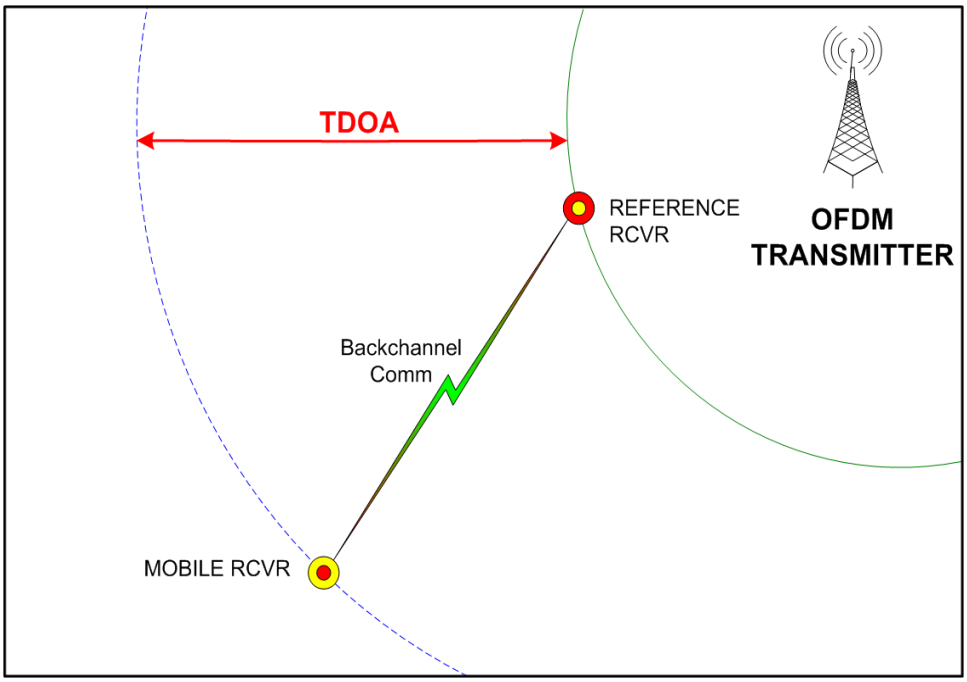

Figure 3.1: System Model. The model consists of one OFDM transmitter and two receivers, the reference and mobile receivers.

For a different notation and better understanding it is possible to represent (3.1) in vector dot product (•) form as follows:

$$R_{rx}(m) = \left[\; y_{rx}(m),\;\; y_{rx}(m+1),\;\ldots\;,\; y_{rx}(m+\nu-1) \;\right] \bullet \begin{bmatrix} y_{rx}(m+N) \\ y_{rx}(m+N+1) \\ \vdots \\ y_{rx}(m+N+\nu-1) \end{bmatrix}^{*} \tag{3.2}$$

where N is the data length of the symbol and ν is the cyclic prefix length. In (3.1) and (3.2), m is the sample index and subscript rx denotes the receiver (i.e., mobile or reference). Essentially, this correlation process takes two "sample windows," both of which are $\nu = 16$ samples wide and are spaced $N = 64$ samples apart, and compares them. When the two windows are aligned with the cyclic prefix and last ν samples of a symbol, (3.1) and (3.2) are at a maximum thus highlighting the boundaries of

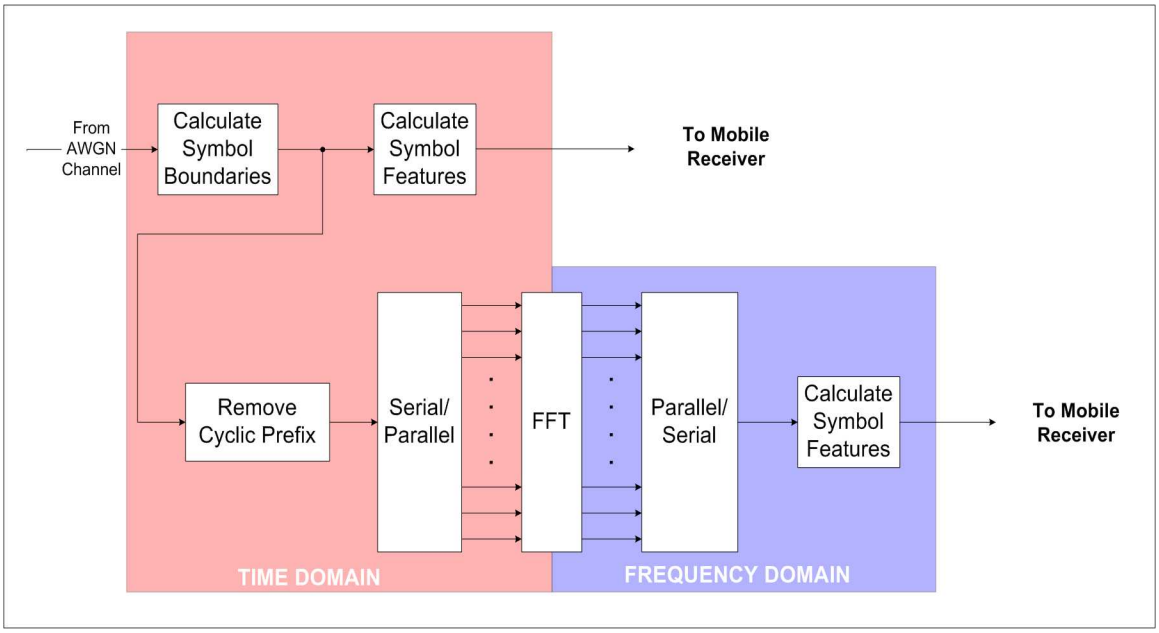

(a) Reference Receiver

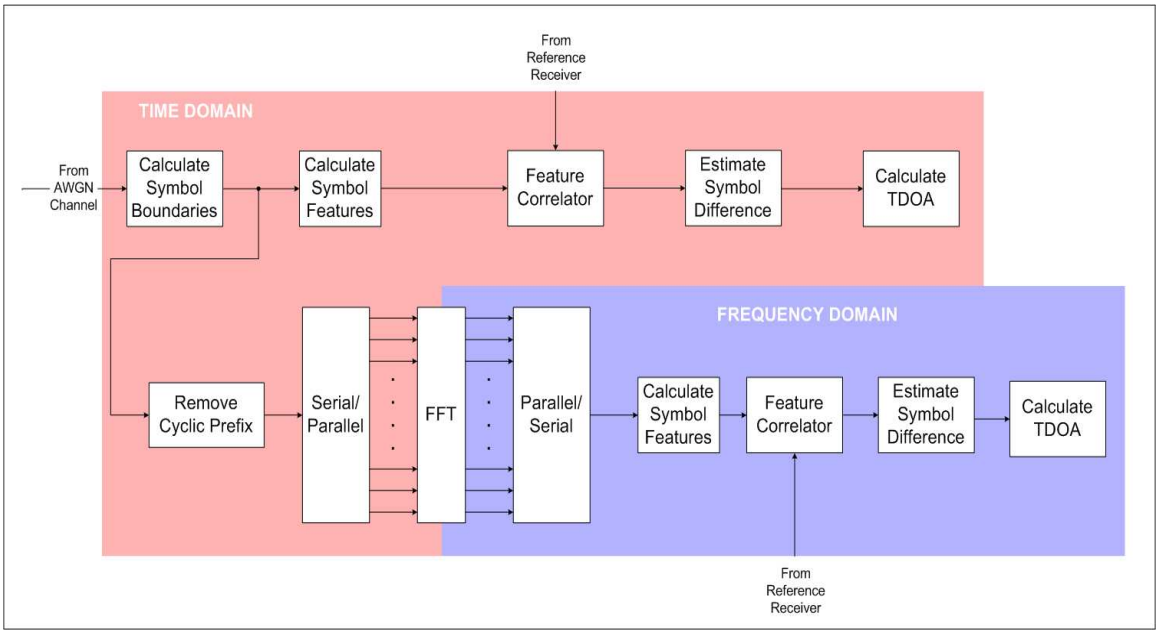

(b) Mobile Receiver

Figure 3.2: Receiver Models. Note that both receivers do the same processes initially, but the mobile receiver does additional signal processing once the reference receiver begins to transmit signal information.

that respective symbol. In other words, compute $R_{rx}(m)$ for all values of m and then look for occurrences of peaks that theoretically should be separated by multiples of $N + \nu$ samples.

Equations (3.3) and (3.4) below give the mathematical expressions for finding individual maximums per symbol and then averaging them over the total number of symobls.

$$\hat{\delta}_{rx} \cong \arg \max_{1 \leq m \leq (N+\nu)} \Re \{\mu_{R_{rx}}(m)\} \tag{3.3}$$

where $\Re\{\spadesuit\}$ is the real portion of $\{\spadesuit\}$ and

$$\mu_{R_{rx}}(m) = \frac{1}{K} \sum_{k=1}^{K} \sum_{i=m+1}^{m+\nu} y_{rx}((N+\nu)k + i) \cdot y_{rx}^{*}((N+\nu)k + i + N) \tag{3.4}$$

where K is a predetermined total number of symbols to average over. For this thesis $K = 2048$ symbols. The averaging technique in (3.4) is a necessary step in order to get a more accurate estimate of the sample shift from the symbol boundary correlator in (3.1).

Figure 3.3 illustrates the simulated results of the symbol boundary correlator using 3.1) over an ideal, no noise channel and an AWGN channel with a +5 dB signal-to-noise ratio (SNR). Notice in Figure 3.3 that the maximum value within each symbol indicates the approximate sample shift from the leftmost symbol boundary. The distance between peaks is approximately 80 samples, which is $(N + \nu)$ the length of a complete symbol in the time domain.

Figure 3.3 also shows that the AWGN channel induces irregularities in the peak correlation values. However, to obtain a more accurate estimate of the true sample shift within a symbol, it is necessary to average the symbol correlation results using (3.4). In other words, the boundary correlation results are partitioned by symbol and all the partitions are averaged together. Think of $R_{rx}(m)$ as vector of K symbols long and each symbol containing M samples. For this thesis $I = 2048$ symbols and $M = 80$

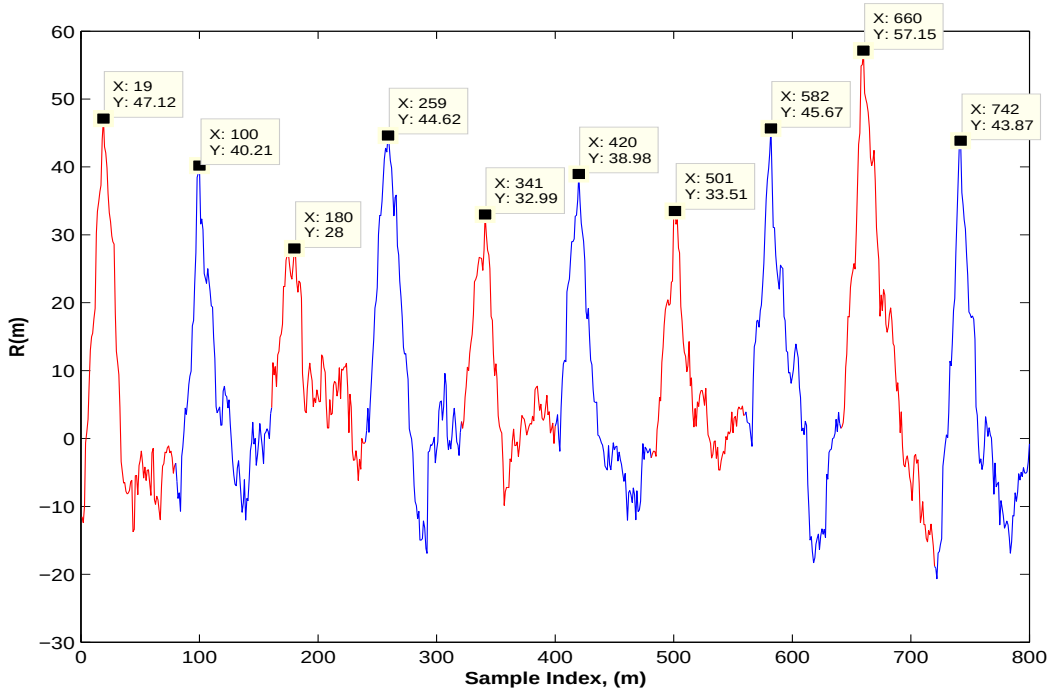

(a) Ideal Channel

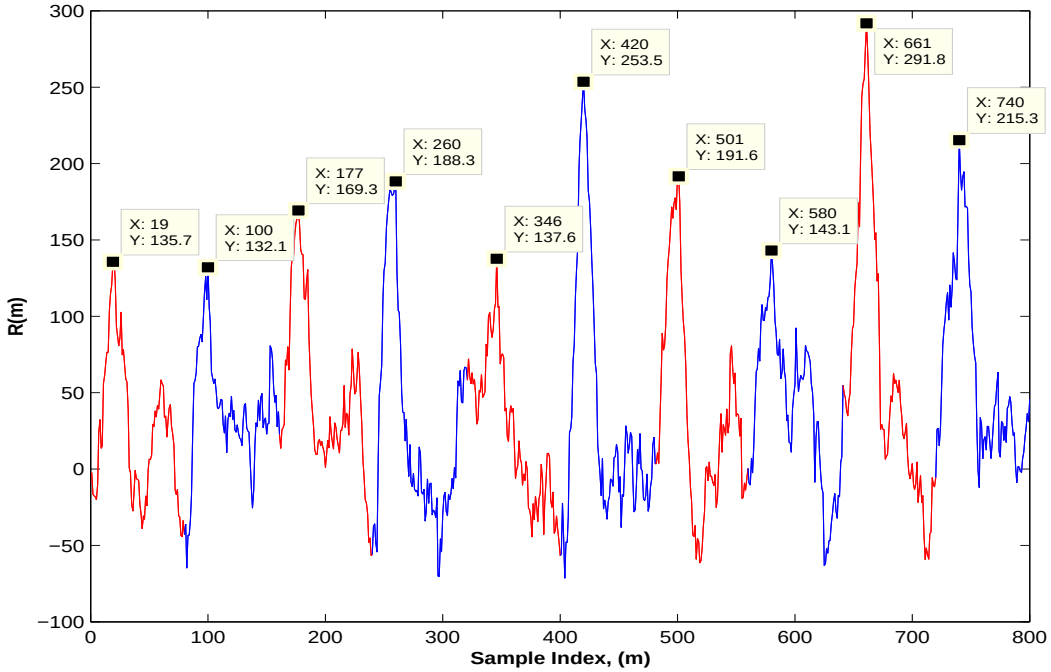

(b) AWGN Channel

Figure 3.3: Symbol Boundary Correlator Results. The alternating colors represent different symbols. Only 10 symbols worth of the received signal are depicted here. (a) SNR = ∞ (b) SNR = +5 dB

samples. In the process of averaging, this vector is decomposed in to a I x M matrix. Ideally, the maximum value of each symbol would be located at the same sample index (m), but since ideal conditions are unobtainable in real channels, averaging the symbols (i.e., the rows of the I x M matrix) will result in an better averaged estimate of the channel delay. Figure 3.4 graphically represents the aforementioned averaging process, and Figure 3.5 shows the averaged results of Figure 3.3. The maximum sample index of the averaged results indicates the sample delay of the received signal. From Figure 3.5, this averaged maximum is 20 samples. Ultimately, this averaging method produces a more accurate estimate of the actual sample shift within a symbol.

Once the sample shift, $\hat{\delta}_{rx}$, has been estimated the entire signal is then shifted by the difference between the sample shift and the total number of samples within a symbol. This shift will then align the received signal on a symbol boundary. The signal is then parsed into symbols per (3.5). This is a necessary step in calculating symbol features in order to determine the symbol shift between receivers.

$$y_{rx}(k) = \begin{bmatrix} y_{rx}(Mk + 1 + \hat{\delta}_{rx}) \\ y_{rx}(Mk + 2 + \hat{\delta}_{rx}) \\ \vdots \\ y_{rx}(Mk + (M-1) + \hat{\delta}_{rx}) \\ y_{rx}(Mk + M + \hat{\delta}_{rx}) \end{bmatrix} \tag{3.5}$$

where subscript rx denotes the specific receiver, either the mobile or reference. $M = N + \nu$ is the total number of samples per symbol, and k identifies a specific symbol. For this research, k is bounded by $1 \leq k \leq 2048$. Finally, $\hat{\delta}_{rx}$ is the average sample shift within a symbol which is determined by the symbol boundary correlation process of (3.3).

! For this thesis all 2048 generated symbols are used in the symbol boundary correlation calculations. The purpose of this thesis is to validate

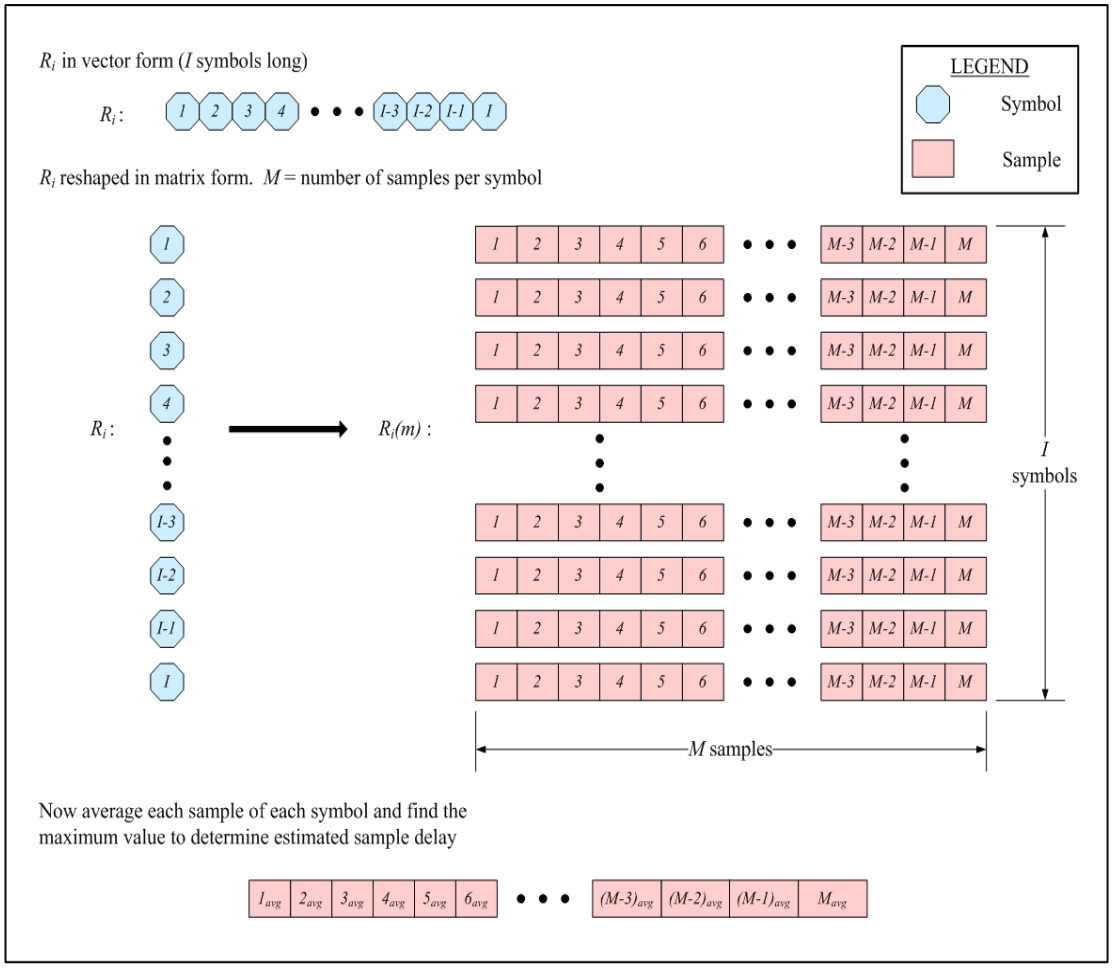

Figure 3.4: Symbol Boundary Correlation Averaging Process. (1) Symbol Boundary Correlator results are broken down into symbols, (2) symbol values are averaged together column-wise, (3) the maximum value of the averaged results corresponds to the sample delay.

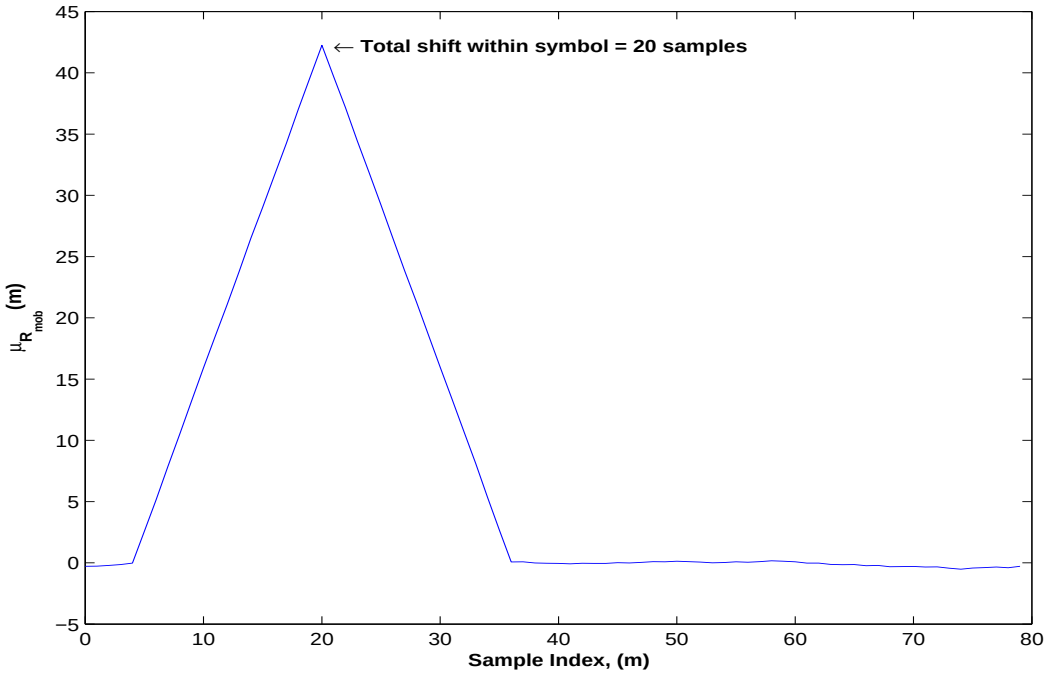

(a) Ideal Channel

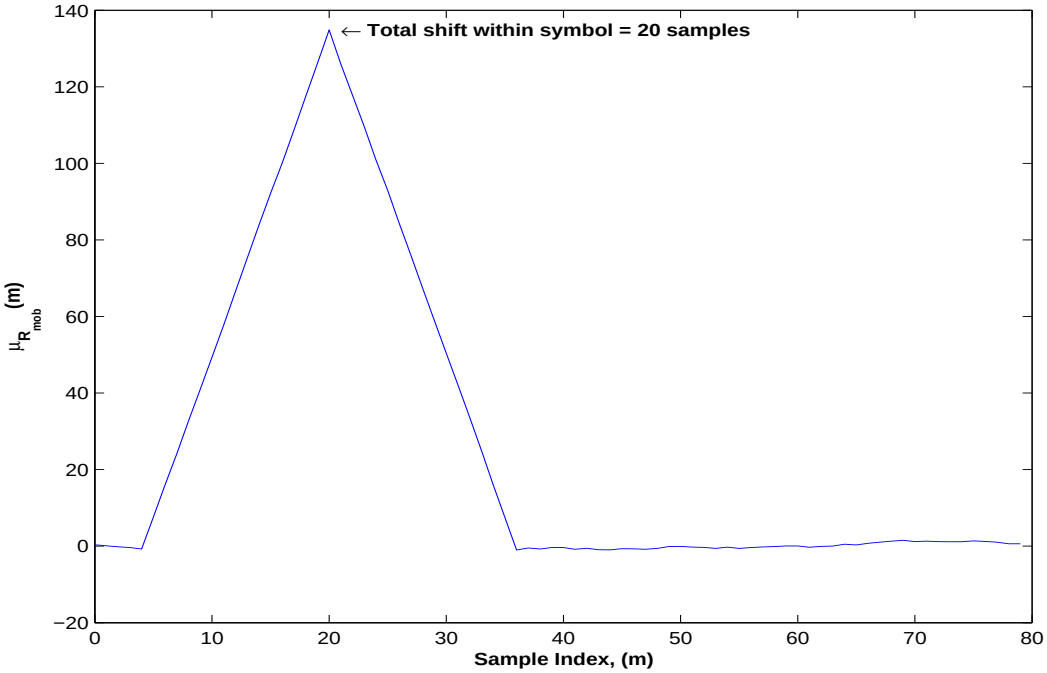

(b) AWGN Channel

Figure 3.5: Averaged Symbol Boundary Correlator Results. For this example, both the ideal and AWGN channel results have been averaged to one symbol as illustrated in Figure 3.4. Notice the single peak. (a) SNR = ∞ (b) SNR = +5 dB

the feature correlation process not the symbol boundary correlations, and increasing the number of symbols to calculate over will in turn increase the accuracy of the symbol boundary correlator estimates.

Using the known repetitive symbol composition of a transmitted OFDM symbol allows for blind symbol boundary detection; therefore, this technique requires no prior knowledge or training signal. The only thing required for this boundary detection process to work is the knowledge that the transmission signal is OFDM and the lengths of N and ν. However, with additional processing the lengths of N and ν could be found non-cooperatively, but for the purposes of this thesis N and ν are predetermined.

3.1.2 Symbol Features. Statistical features are calculated for each symbol in both the time and frequency domains. The following is a list of features considered. These features were selected for convenience and initial proof-of-concept. There was no presupposition of optimality nor any prior related work to guide in feature selection.

- *Mean:* (1^{st} Moment)

$$\mu_{rx}(k) = \frac{1}{M'} \sum_{i=1}^{M'} y_{rx}(M'k + i + \hat{\delta}_{rx}) \tag{3.6}$$

- *Variance:* (2^{nd} Moment)

$$\sigma^2_{rx}(k) = \frac{1}{M'-1} \sum_{i=1}^{M'} \left| y_{rx}(M'k + i + \hat{\delta}_{rx}) - \mu_{rx}(k) \right|^2 \tag{3.7}$$

- *Skewness:* (3^{rd} Moment)

$$\gamma_{1_{rx}}(k) = \frac{1}{\left(\sqrt{\sigma^2_{rx}(k)}\right)^3 \ (M'-1)} \sum_{i=1}^{M'} \left| y_{rx}(M'k + i + \hat{\delta}_{rx}) - \mu_{rx}(k) \right|^3 \tag{3.8}$$

- *Kurtosis:* (4^{th} Moment)

$$\gamma_{2_{rx}}(k) = \frac{1}{\left(\sqrt{\sigma^2_{rx}(k)}\right)^4 \ (M'-1)} \sum_{i=1}^{M'} \left| y_{rx}(M'k+i+\hat{\delta}_{rx}) - \mu_{rx}(k) \right|^4 \tag{3.9}$$

- *Standard Deviation:*

$$\sigma_{rx}(k) = \sqrt{\frac{1}{M'-1} \sum_{i=1}^{M'} \left| y_{rx}(M'k+i+\hat{\delta}_{rx}) - \mu_{rx}(k) \right|^2} \tag{3.10}$$

- *Peak-to-Average Power Ratio:*

$$PAPR_{rx}(k) = \frac{\max_{1 \le i \le M'} \left| \left(y_{rx}(M'k+i+\hat{\delta}_{rx}) - \mu_{rx}(k) \right) \right|^2}{\frac{1}{M'} \sum_{i=1}^{M'} \left| \left(y_{rx}(M'k+i+\hat{\delta}_{rx}) - \mu_{rx}(k) \right) \right|^2} \tag{3.11}$$

- *Average Symbol Phase:*

$$\Phi_{rx}(k) = \arctan \left[\frac{\sum_{i=1}^{M'} Im \left(y_{rx}(M'k+i+\hat{\delta}_{rx}) - \mu_{rx}(k) \right)}{\sum_{i=1}^{M'} Re \left(y_{rx}(M'k+i+\hat{\delta}_{rx}) - \mu_{rx}(k) \right)} \right] \tag{3.12}$$

- *Root-Mean-Squared:*

$$RMS_{rx}(k) = \sqrt{\frac{1}{M'} \sum_{i=1}^{M'} \left(y_{rx}(M'k+i+\hat{\delta}_{rx}) - \mu_{rx}(k) \right)^2} \tag{3.13}$$

The value of M' depends on the domain in which the calculations are made. In the time domain M' equals $N + \nu$ samples, and for the frequency domain M' is simply N.

From Figure 3.2, there is additional signal conditioning that is accomplished before the features are calculated in the frequency domain. Specifically, the cyclic

prefix is removed and a FFT is performed. The cyclic prefix is removed so that the FFT length, N, matches that of the IFFT in the transmitter. Also, the FFT is the critical operation which converts the signal from the time domain to the frequency domain.

3.1.3 Symbol Feature Correlator. After the reference receiver has calculated the symbol features per (3.6) - (3.13), it transmits those features to the mobile receiver via the backchannel communications link. Once the mobile receiver collects a predetermined number of feature calculations (i.e., "window size") from the reference receiver, it then begins the correlation process. The more reference features gathered, the better the symbol shift estimates will be because the mobile has a larger sample set to compare its features with. The effects of varying the "window size" on the symbol shift estimations is discussed in the next chapter. *"Window size"* will be the term used for the remainder of this thesis to refer to the number of features, K, collected by the mobile from the reference. The following algorithm is used at the mobile receiver to compute the feature correlations:

$$\hat{R}_F(m) = \sum_{k=1}^{K} \left(f_{ref}(k) - \mu_{f_{ref}(1)}\right) \cdot \left(f_{mob}(k+m) - \mu_{f_{mob}(1+m)}\right)^* \tag{3.14}$$

where

$$\mu_{f_{rx}}(n) = \frac{1}{K} \sum_{i=n}^{K+n-1} f_{rx}(i) \tag{3.15}$$

Window size N_F in (3.14) and (3.15) is the number of symbols worth of features collected by the mobile from the reference receiver, and $\mu_{f_{rx}}$ is the mean of a desired feature from the rx receiver (i.e., the mobile or reference receiver). The variable n in (3.15) denotes the starting symbol of the feature window. For simulations in this research $n = 256$; therefore, the actual reference features that correlate with the mobile features start at symbol 256 and end at the symbol $256 + K - 1$.

The mobile receiver computes (3.14) for all anticipated valid ranges of the symbol arrival time difference, $-D \leq d \leq D$. For this research $D = 100$, which indicates the maximum possible symbol difference between the two receivers can be no more than $\pm D$ symbols. In other words, the mobile receiver must calculate $K+2D$ symbols worth of features; whereas, the reference receiver only needs to calculate K worth. Below is the expression for the symbol difference between the mobile and reference receivers.

$$\Delta_{Symbol} = \arg \max_{-D \leq d \leq D} \Re \left\{ \hat{R}_F(d) \right\} \tag{3.16}$$

The sign of index d in (3.16) is very important since it indicates which of the two receivers "saw" the transmitted signal first. For example, if d is negative, the mobile receiver received the transmission before the reference which means the mobile is closer to the transmitter than the reference receiver. The opposite is true for positive d. Figure 3.6 depicts both a positive and negative index d in (3.16).

For the variance, standard deviation, PAPR, and RMS feature correlations it was necessary to filter the results using a second-order differential filter to better interpret the respective correlation maximums. The peaks on the unfiltered correlations are not as predominant as the filtered results. Therefore, this second-order differential filter is designed to highlight amplitude changes between sequential samples. It was implemented simply by convolving the unfiltered correlation results with the array $[-1, \ \ 2, \ \ -1]$, which is a high-pass filter.

3.2 TDOA Calculations

Calculating the TDOA measurement between two received OFDM signals is accomplished using:

$$TDOA_{OFDM} = (\delta_{Sample} + (N + \nu) \cdot \Delta_{Symbol}) \cdot T_{samp} \tag{3.17}$$

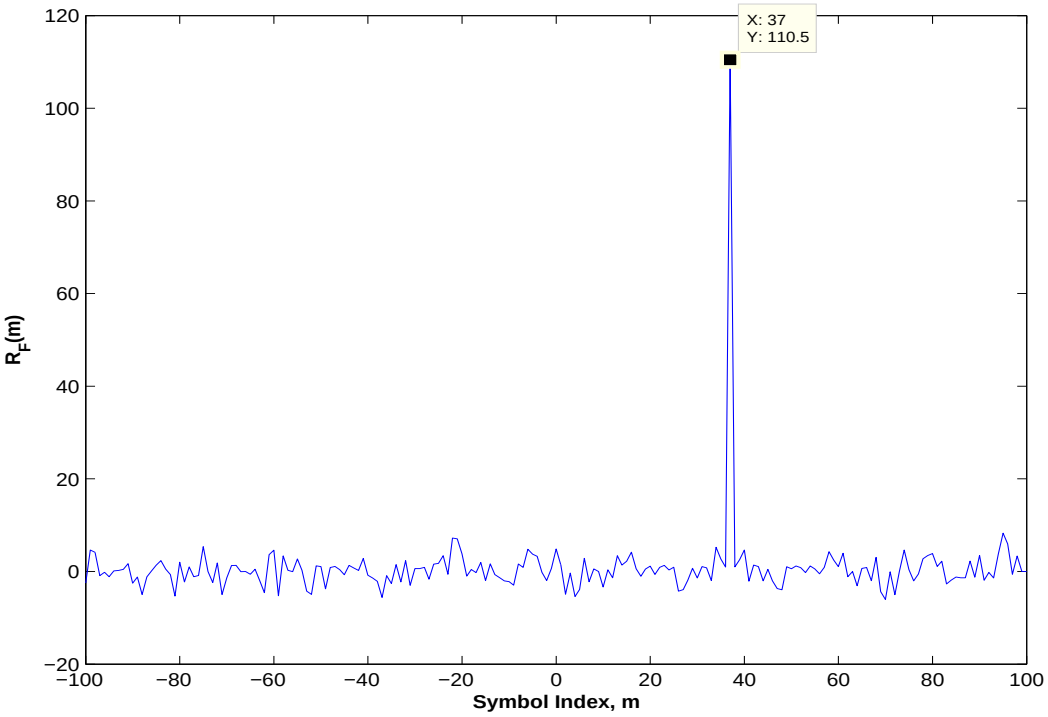

(a) Positive d

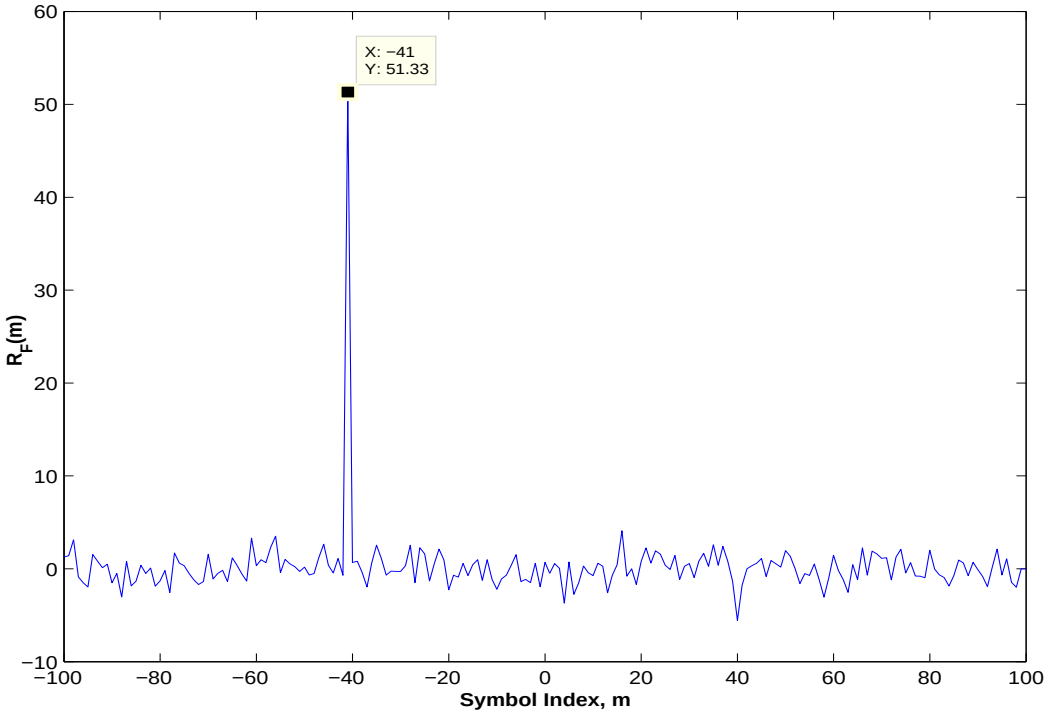

(b) Negative d

Figure 3.6: Symbol Difference, Δ_{Symbol}, Peak. Notice the index sign where the maximum occurs. (a) Positive feature correlator index (b) Negative feature correlator index

Table 3.1: TDOA Units.

Variable	Units
Δ_{Sample}	$Samples$
$N+\nu$	$\frac{Samples}{Symbol}$
Δ_{Symbol}	$Symbols$
T_{samp}	$\frac{Seconds}{Sample}$

where δ_{Sample} is the difference in reception times of the symbol boundaries given in samples. This can be mathematically expressed as the location of the average maximum value of the mobile receiver boundary correlator minus the average maximum value location of the reference receiver boundary correlator, expressed as:

$$\delta_{Sample} = \hat{\delta}_{ref} - \hat{\delta}_{mob} \tag{3.18}$$

The Δ_{Symbol} term in (3.17) is the symbol difference between the two receivers and is the estimated location of the maximum value of the feature correlator at the mobile receiver. For simulations, $N = 64$ samples and $\nu = 16$ samples. Finally, T_{samp} is the sampling period.

Equation (3.17) was derived simply by using unit analysis. Knowing that TDOA is a measure of time, it is possible to derive a complete TDOA expression which was implemented for the OFDM signaling in this research. Table 3.1 shows the units for each variable in (3.17). Note that Δ_{Symbol} is converted from symbols to samples in order for (3.17) to yield the appropriate unit of time (seconds). There are 80 $\frac{samples}{symbol}$; which is necessary for the conversion process.

One important fact to gather from (3.14) and (3.17) is that Δ_{Symbol} is directly related to K which in turn effects TDOA calculations. The larger K the longer the receivers must wait in real-time to collect K symbols. This collection time effects TDOA estimations. For example, for a stationary mobile receiver this collection time would be practically irrelevant since the position is not changing. However, for a

moving object, say an aircraft traveling at the speed of sound, this collection time would greatly effect current TDOA estimates. Therefore, in practice it is desirable to keep K as small as possible to maintain desired TDOA accuracy. *Chapter IV* discusses the effects of varying the *window size* at given SNRs.

3.3 Summary

This chapter describes the overall transmitter-receiver system model and parameters needed to evaluate the correlator outputs for the OFDM receivers for the purpose of navigation. Additionally, it was discussed how symbol features were used for TDOA measures. This chapter also discussed the relationship between the reference receiver with the mobile receiver when comparing those symbol features. The term *"window size"* was also introduced/defined in order to clarify conclusions drawn from *Chapter IV* findings.

IV. Research Results

This chapter presents the simulated results for the transmitter-receiver model detailed in Chapter III. Specifically, the effectiveness of the feature correlator is evaluated in Section 4.1. Finally, an overall summary is given of the findings.

4.1 Feature Correlator Simulation Results

This section explains the effects on the symbol feature correlator described in Section 3.1.3 when the AWGN channel's SNR values and feature correlator window size are varied. The SNR values for the AWGN channel are varied from -20 dB to 40 dB in 1 dB steps, and the window sizes evaluated are 10, 100, 250, 500, 750, and 1000 symbols.

The feature correlator performance is measured by evaluating P_{Error}, the probability that an error occurred in Δ_{Symbol} estimation. Equation (4.1) gives a mathematical expression for P_{Error}.

$$P_{Error} = P\left[\hat{\Delta}_{Symbol} \neq \Delta_{Symbol}\right] \tag{4.1}$$

where $\hat{\Delta}_{Symbol}$ is the actual symbol difference between the mobile and reference receivers, and Δ_{Symbol} is the estimated symbol difference per (3.16).

P_{Error} is calculated using a hard-decision method. In other words, if the symbol correlator did not *exactly* determine the actual symbol shift then it is recorded as an error. There is no tolerance region or threshold implemented for a correct estimate. However, since all simulations are conducted in discrete time, there is an implicit tolerance region which is less than $\pm$ 1 sample.

Notice from Figures 4.1 - 4.8 that the time domain correlation results are marginally better than those from the frequency domain. Remember from the receiver block diagram in Figure 3.1 that the cyclic prefix is removed from the symbol before the feature correlation process occurs in the frequency domain. This removal

process takes away $\nu = 16$ samples from each symbol thus reducing the total number of samples per symbol from $M = N + \nu = 80$ to simply $N = 64$. This sample reduction causes the accuracy of the correlation process to decrease by condensing the comparison samples. For this reason the following discussions will focus only on the time domain results.

Another important fact to note is that the *window size* also effects the feature correlator's performance. Remember from (3.14) that the maximum bound of the summation is determined primarily by the *window size*. Therefore, as the *window size* increases so does the number of symbol features being compared and thus the correlator's performance improves. See Figures 4.1 - 4.8 for reference.

4.1.1 Mean Feature Correlator. Figure 4.1 shows the average results for 1000 trials for the mean feature correlator in the time and frequency domains. Evaluating the correlation window size of 100 symbols in the time domain as a baseline (window size arbitrarily chosen for discussion purposes), the P_{Error} begins to significantly increase when the SNR values decrease below approximately -4.5 dB. Table 4.1 shows that for a window size of 100 symbols there is a 40% decrease in the mean feature correlator effectiveness in approximately a 2.37 dB decrease in SNR (-5.37 dB to -7.74 dB). However, the mean feature correlator is better than 3.5% effective when the channel's SNR is greater than -4.5 dB.

4.1.2 Variance Feature Correlator. The average results for 1000 trials for the variance feature correlator in the time and frequency domains is illustrated in Figure 4.2. Again, the P_{Error} begins to significantly increase as the SNR values decrease below approximately 5 dB for a correlation *window size* of 100 symbols in the time domain.

4.1.3 Standard Deviation Feature Correlator. Figure 4.5 depicts the average results for 1000 trials for the standard deviation feature correlator in both the time

Table 4.1: Mean Feature Correlator Performance in the Time Domain.

Correlator Window Size	**SNR(dB) at 50% P_{Error}**	**SNR(dB) at 20% P_{Error}**	**SNR(dB) at 10% P_{Error}**
10	0.33	3.60	5.31
100	-7.74	-6.12	-5.37
250	-9.90	-8.62	-8.03
500	-11.69	-10.17	-9.50
750	-12.66	-11.23	-10.56
1000	-13.30	-11.89	-11.21

and frequency domains. For a correlation *window size* of 100 symbols the P_{Error} in the time begins to significantly increase as the SNR values decrease below approximately 5 dB. Notice from Figure 4.9 that the variance and standard deviation have nearly the exact same P_{Error} for the entire SNR range. This may be cause by the close mathmatical relationship between the two features. Remember from (3.7) and (3.10) that standard deviation is nothing more than the square root of variance.

4.1.4 Skewness and Kurtosis Feature Correlators. The skewness and kurtosis feature correlation results in Figures 4.3 and 4.4 show that the P_{Error} is extremely poor for nearly the entire SNR region evaluated. Only when the *window size* increases above 250 and the SNR is 35 dB for skewness does the P_{Error} reach below about 12%; however, for the kurtosis feature correlator the best P_{Error} is about 13% at a SNR of 40 dB. Notice that for both the skewness and kurtosis correlators that P_{Error} does not to appear to get any better once the *window size* reaches or surpasses a size of 500 symbols. One explanation for such poor performance may be that both skewness and kurtosis are such high order statistics that more data (i.e., a *window size* greater than 1000 symbols) may be required for a more accurate symbol estimation.

Table 4.2: Phase Feature Correlator Performance in the Time Domain.

Correlator Window Size	**SNR(dB) at 50% P_{Error}**	**SNR(dB) at 20% P_{Error}**	**SNR(dB) at 10% P_{Error}**
10	11.70	33.42	N/A
100	-1.89	0.60	1.74
250	-4.78	-3.01	-2.04
500	-6.67	-4.90	-4.07
750	-7.66	-6.15	-5.35
1000	-8.34	-6.78	-6.12

4.1.5 Peak-to-Average Power Feature Correlator. In Figure 4.6, the average for 1000 trials for the PAPR feature correlator illustrates that the P_{Error} begins to significantly increase as the SNR values fall below approximately 8 dB for a correlation *window size* of 100 symbols in the time domain.

4.1.6 Average Symbol Phase Feature Correlator. The average P_{Error} for 1000 trials for the symbol phase feature correlator in the time and frequency domains is depicted in Figure 4.7. Notice that the P_{Error} begins to significantly increase as the SNR values decrease below approximately 3 dB for a correlation *window size* of 100 symbols in the time domain. Table 4.2 shows that for a window size of 100 symbols there is a 40% decrease in the feature correlator effectiveness in approximately a 3.63 dB decrease in SNR (1.74 dB to -1.89 dB). However, the phase feature correlator is better than 3% effective when the channel's SNR is greater than 3.83 dB evaluated with a *window size* of 100.

!

4.1.7 Root-Mean-Squared Feature Correlator. Figure 4.8 represents the average results for 1000 trials for the RMS feature correlator in the time and frequency domains. The P_{Error} begins to significantly increase as the SNR values fall below

approximately 2.75 dB for a correlation *window size* of 100 symbols in the time domain.

4.2 Summary

From Figures 4.1 - 4.8 it is apparent that some feature correlators perform better at lower SNR values than others. The features examined in this research are ranked below according to performance at lower SNR values:

1. Mean
2. Phase
3. Root Mean Squared
4. Variance and Standard Deviation
5. Peak to Average Power Ratio
6. Skewness
7. Kurtosis

Figure 4.9 graphically illustrates the above list with a *window size* of 100. From this figure and the above list, it is easy to see that the mean feature is the best performing feature at lower SNR values. This may be due to the fact that both symbol phase and magnitude are preserved in the actual calculations (see (3.6)). Also, notice that the results for variance and standard deviation are nearly equal for the entire evaluated SNR range. This may be due to the fact that variance is derived from the standard deviation (see (3.7) and (3.10)). Additionally, the PAPR is one of the worst three features (just outperforming skewness and kurtosis). This may due to the fact that PAPR of an OFDM signal is very sensitive to maximum outliers since the numerator of (3.11) requires the maximum peak of the signal squared. Therefore, if noise distorts the signal to the point where a "false" maximum occurs, then the PAPR becomes an erroneous feature. Finally, from this research it is possible to

conclude when using this OFDM model that both the skewness and kurtosis features are unusable for TDOA calculations. Since these are higher order statistics, they possibly may require more data for accurate estimations.

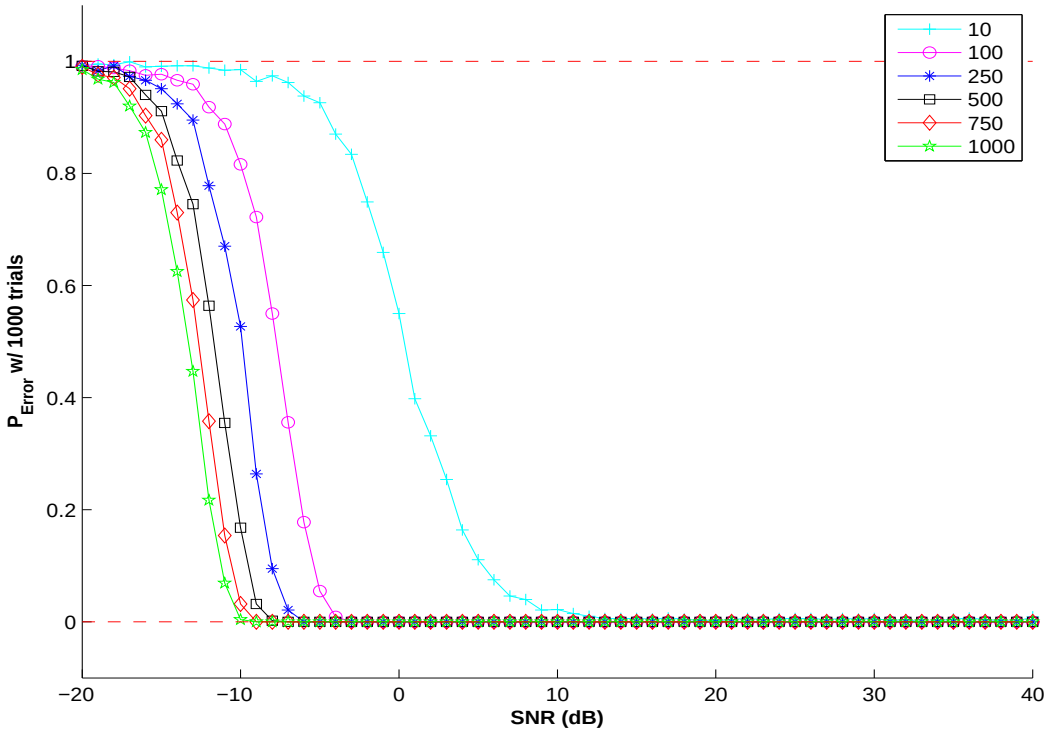

(a) Time Domain

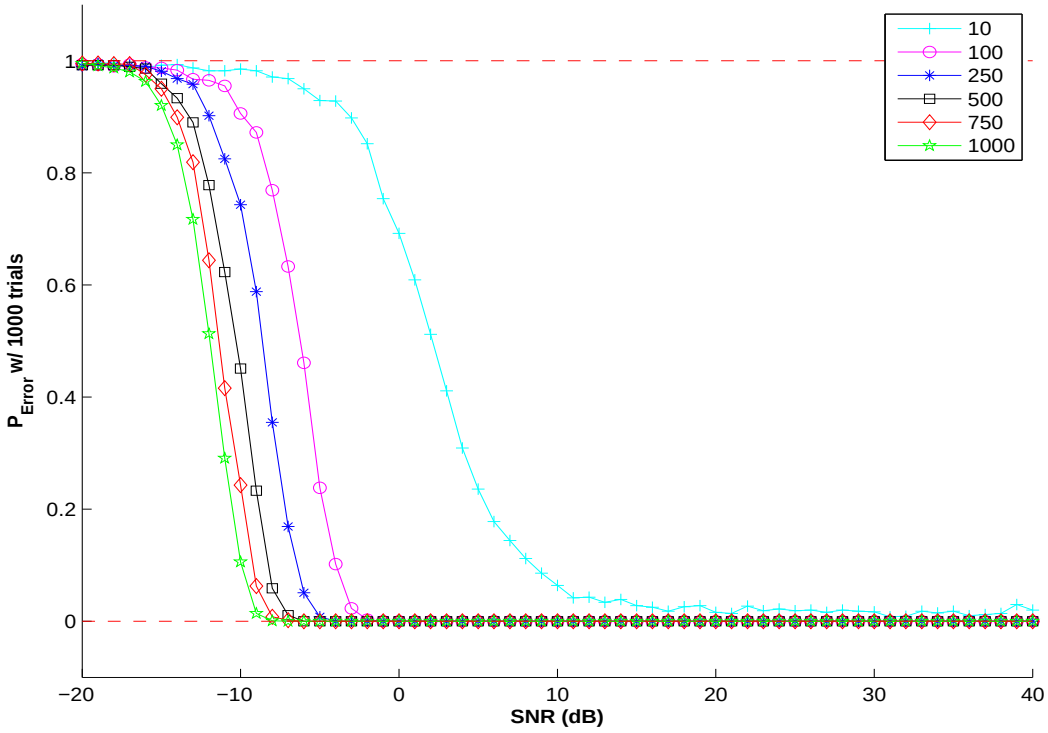

(b) Frequency Domain

Figure 4.1: Feature (MEAN) correlation results averaged over 1000 trials. (a) Time Domain (b) Frequency Domain

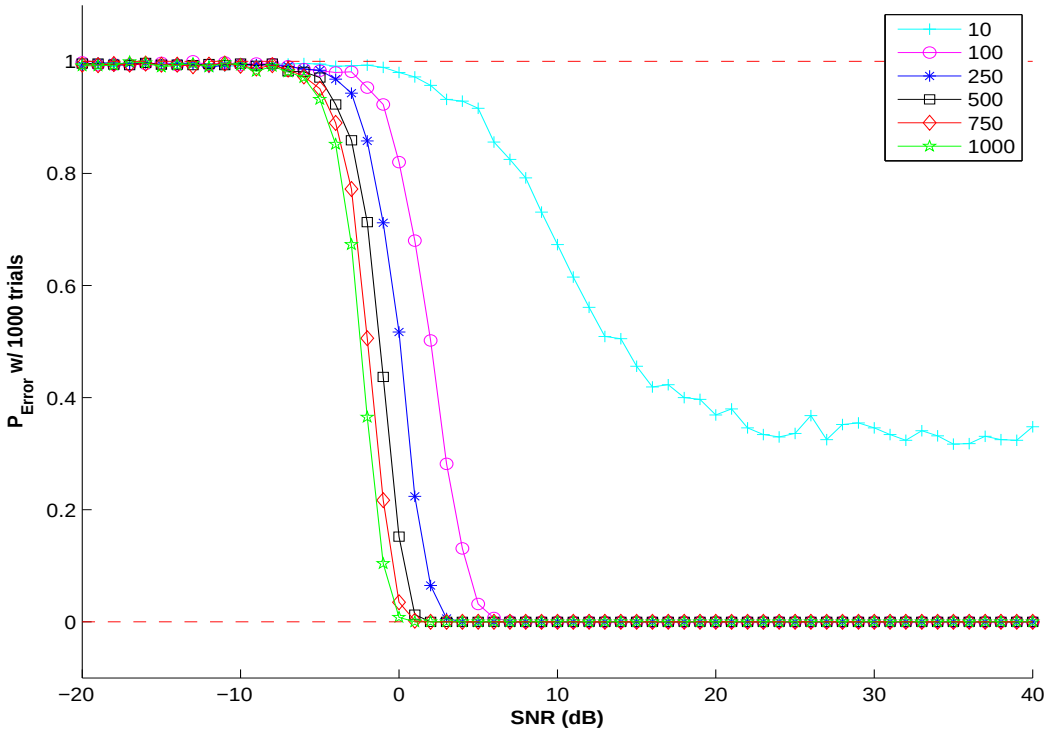

(a) Time Domain

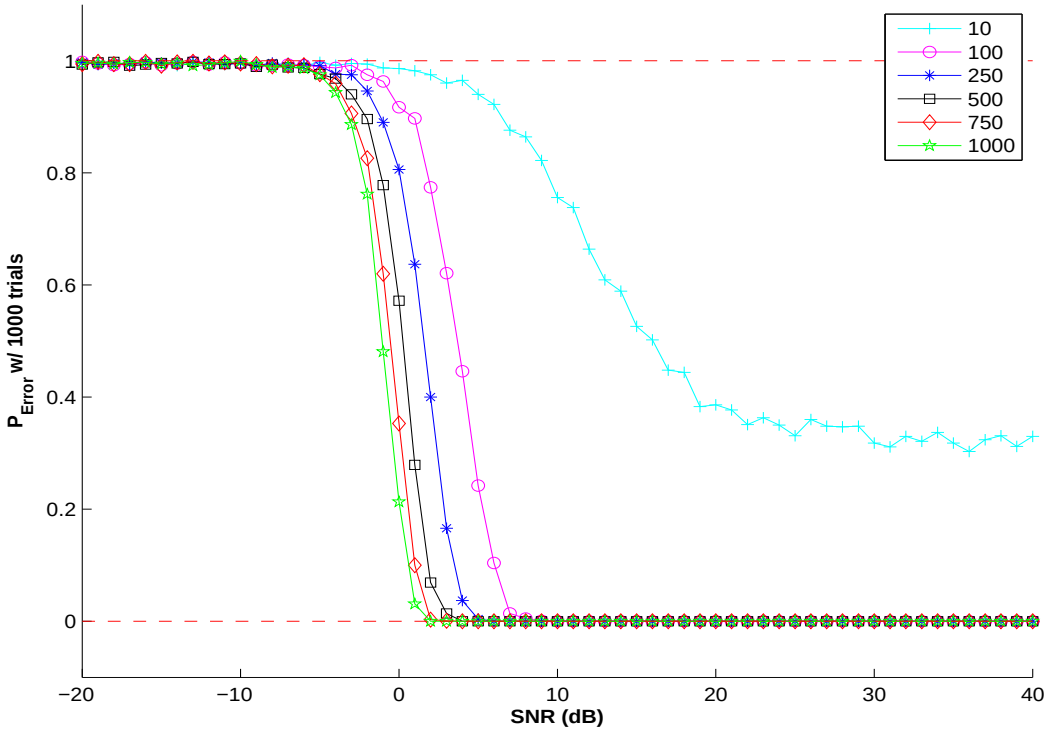

(b) Frequency Domain

Figure 4.2: Feature (VARIANCE) correlation results averaged over 1000 trials. (a) Time Domain (b) Frequency Domain

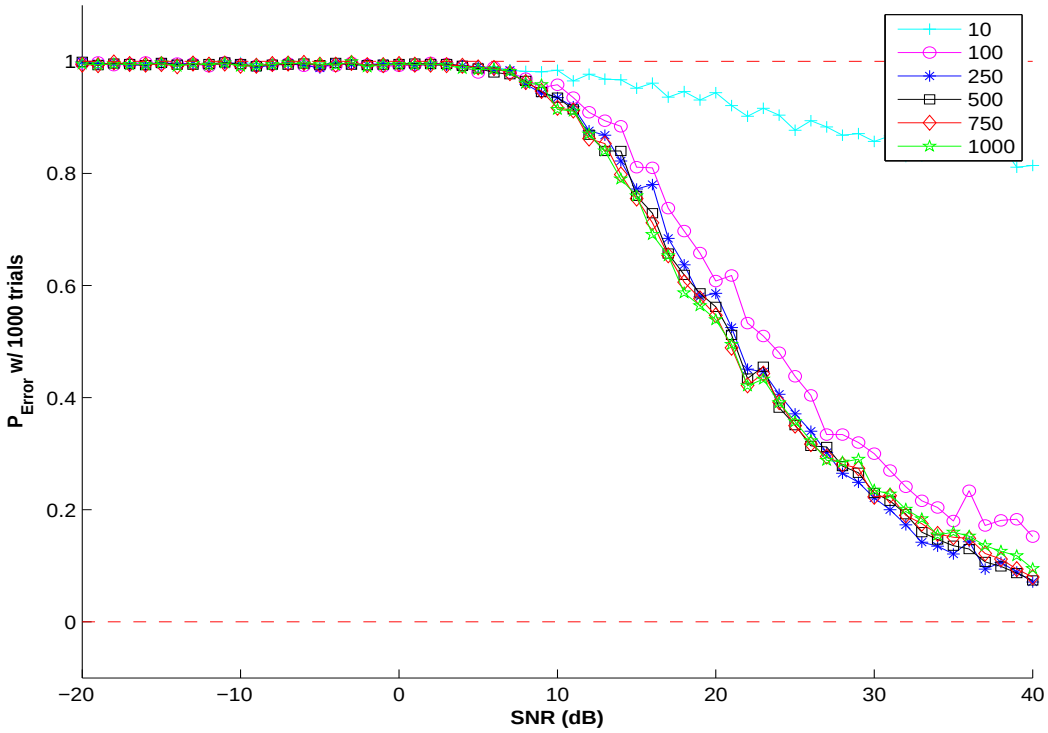

(a) Time Domain

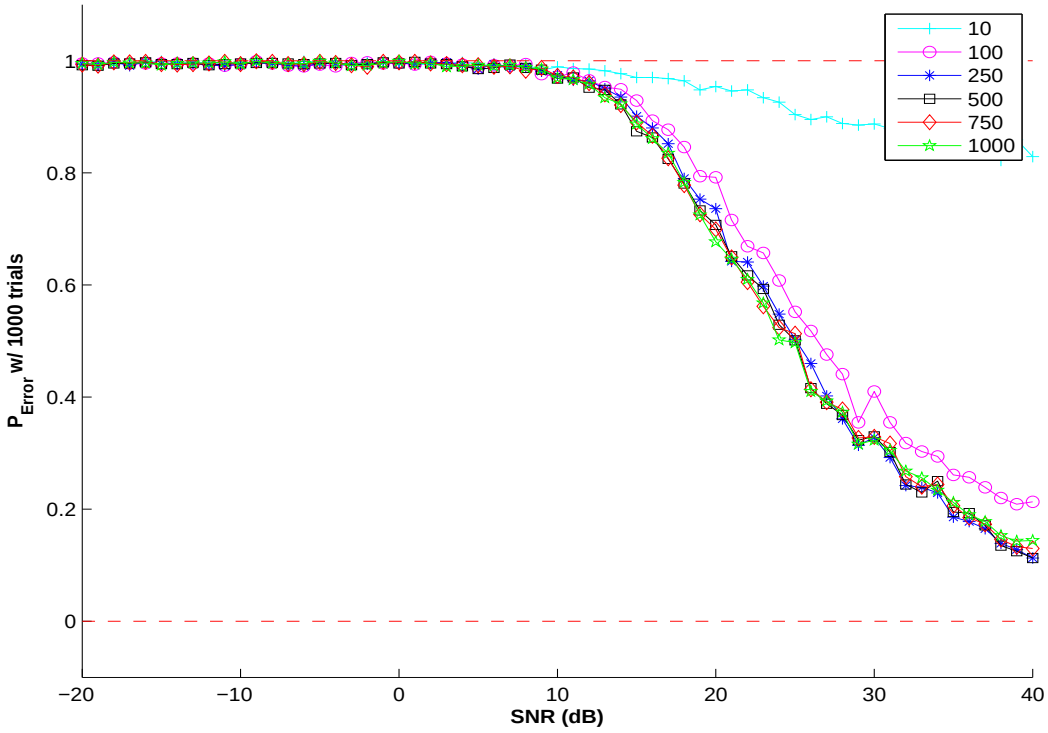

(b) Frequency Domain

Figure 4.3: Feature (SKEWNESS) correlation results averaged over 1000 trials. (a) Time Domain (b) Frequency Domain

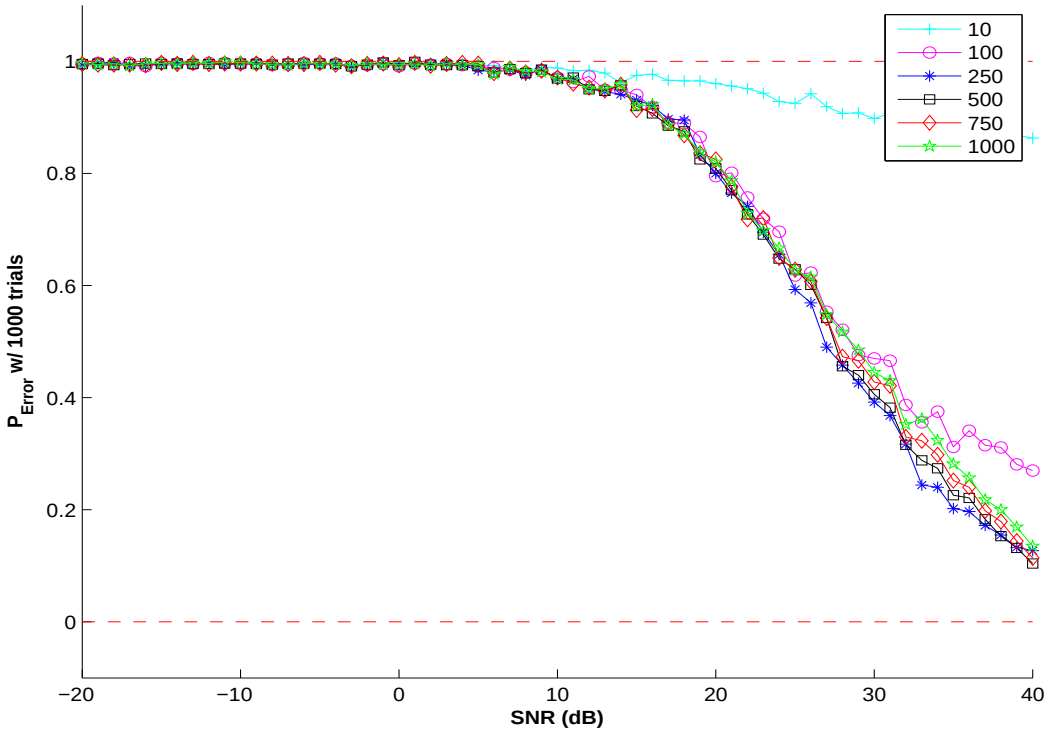

(a) Time Domain

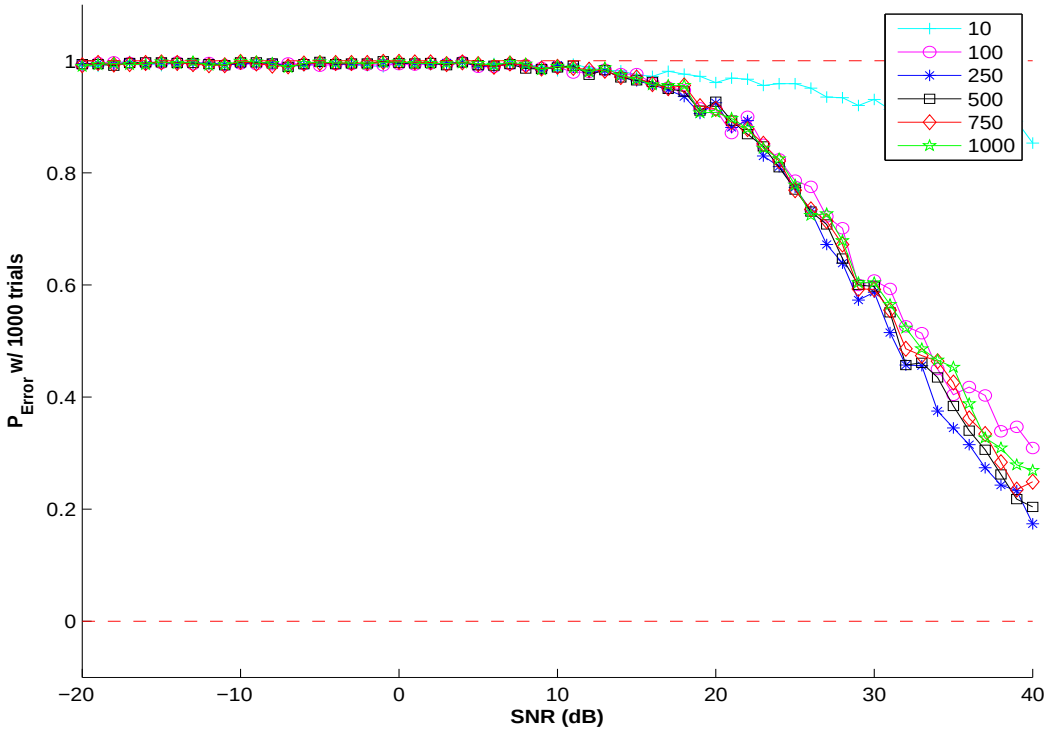

(b) Frequency Domain

Figure 4.4: Feature (KURTOSIS) correlation results averaged over 1000 trials. (a) Time Domain (b) Frequency Domain

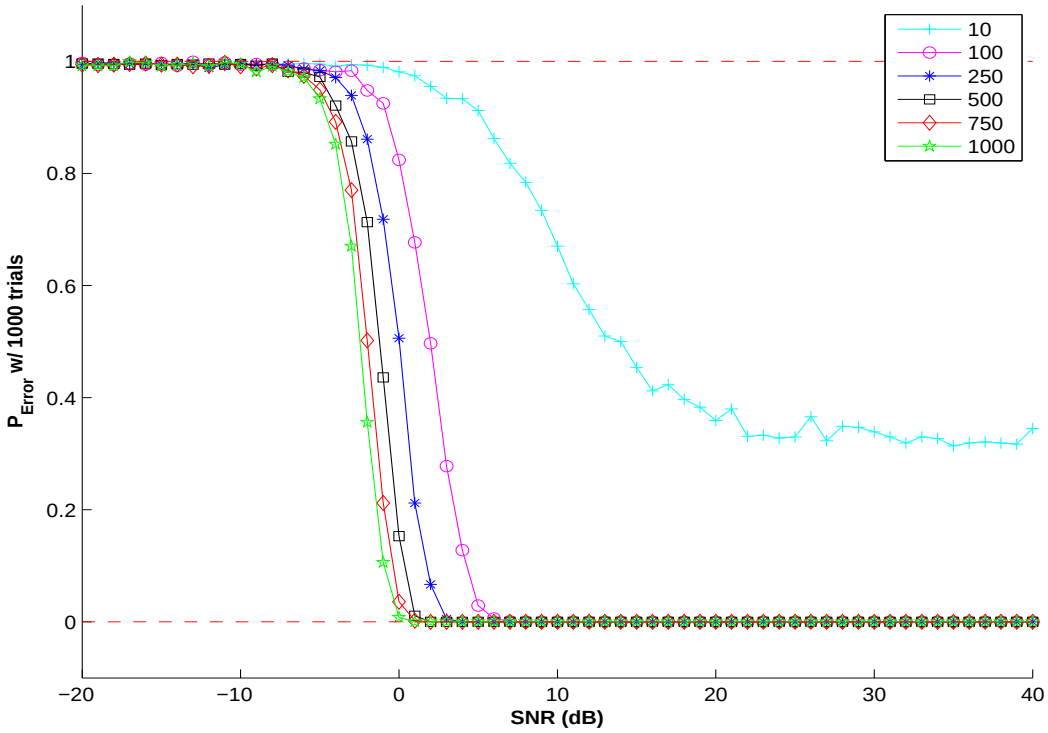

(a) Time Domain

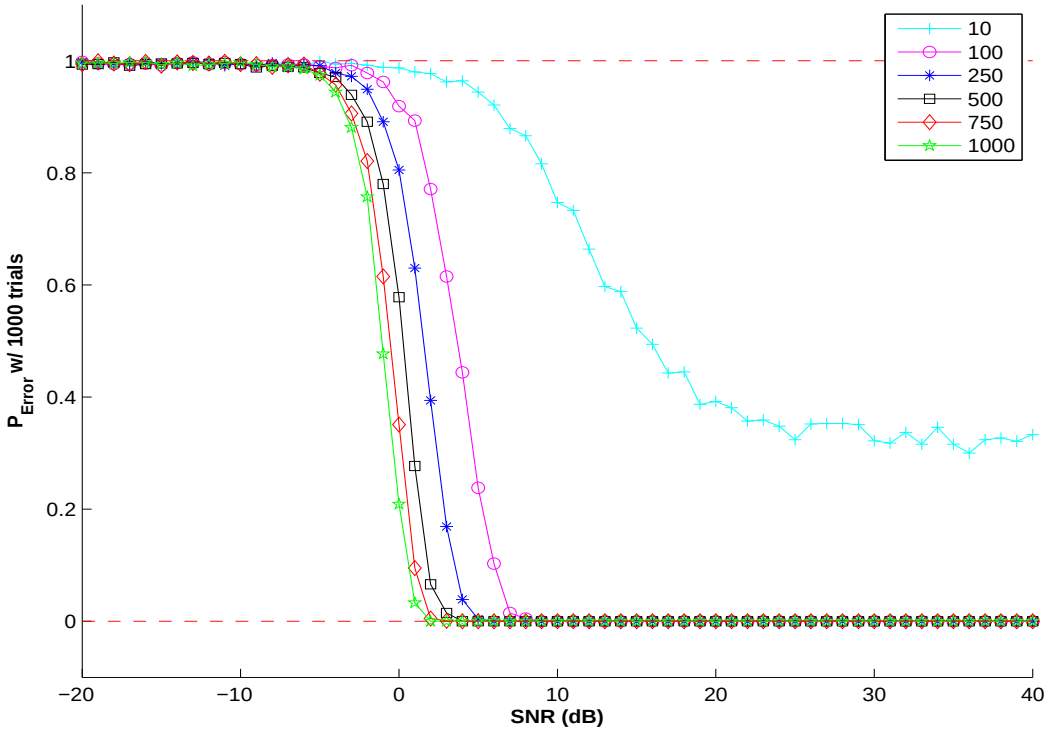

(b) Frequency Domain

Figure 4.5: Feature (STANDARD DEVIATION) correlation results averaged over 1000 trials. (a) Time Domain (b) Frequency Domain

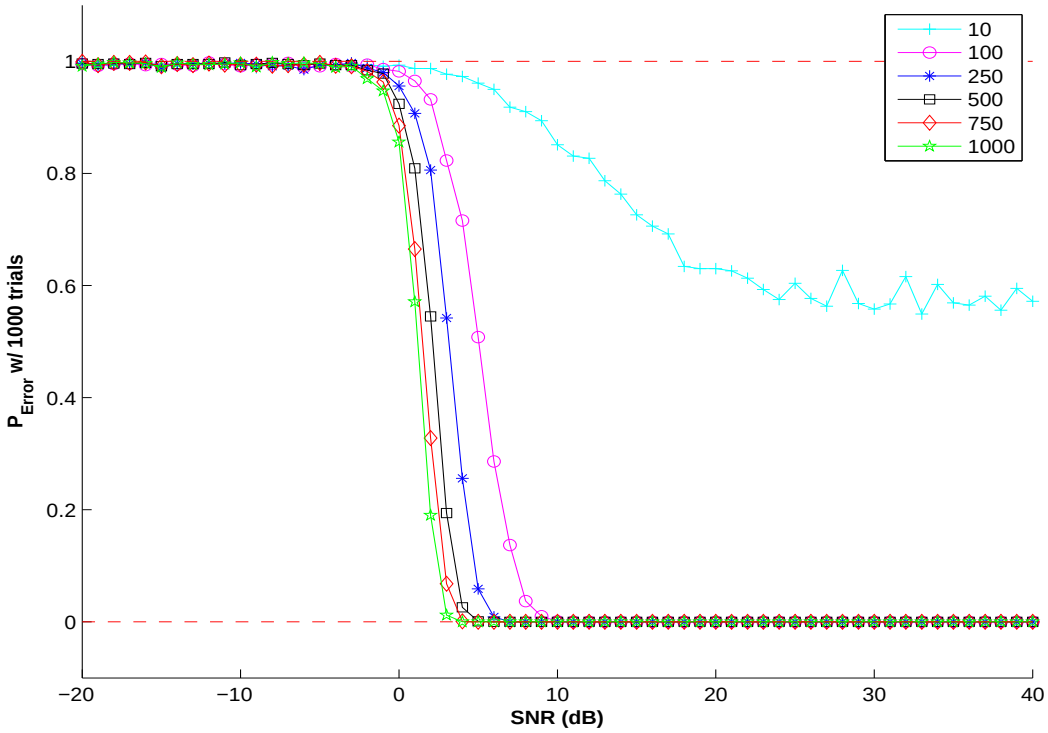

(a) Time Domain

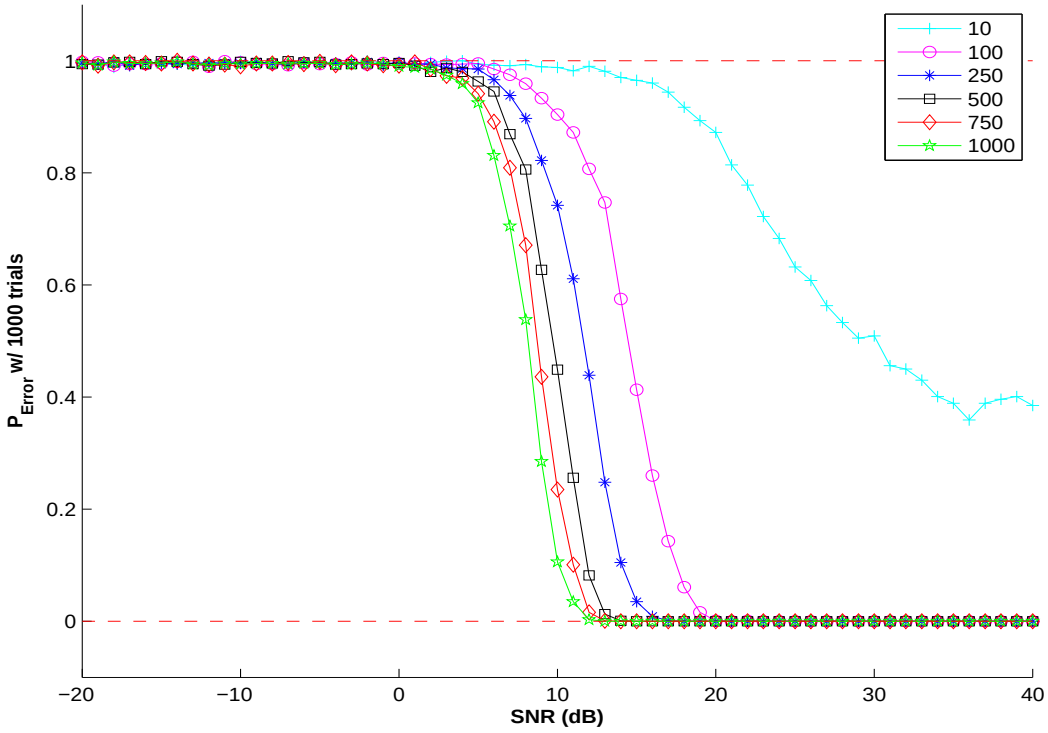

(b) Frequency Domain

Figure 4.6: Feature (PAPR) correlation results averaged over 1000 trials. (a) Time Domain (b) Frequency Domain

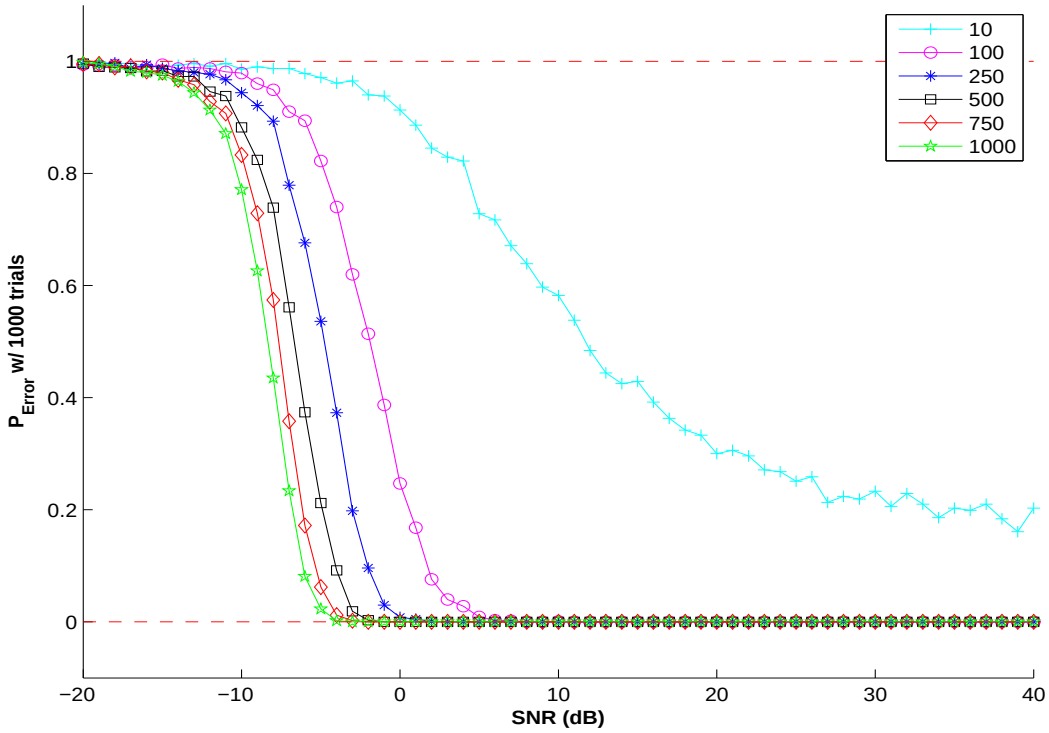

(a) Time Domain

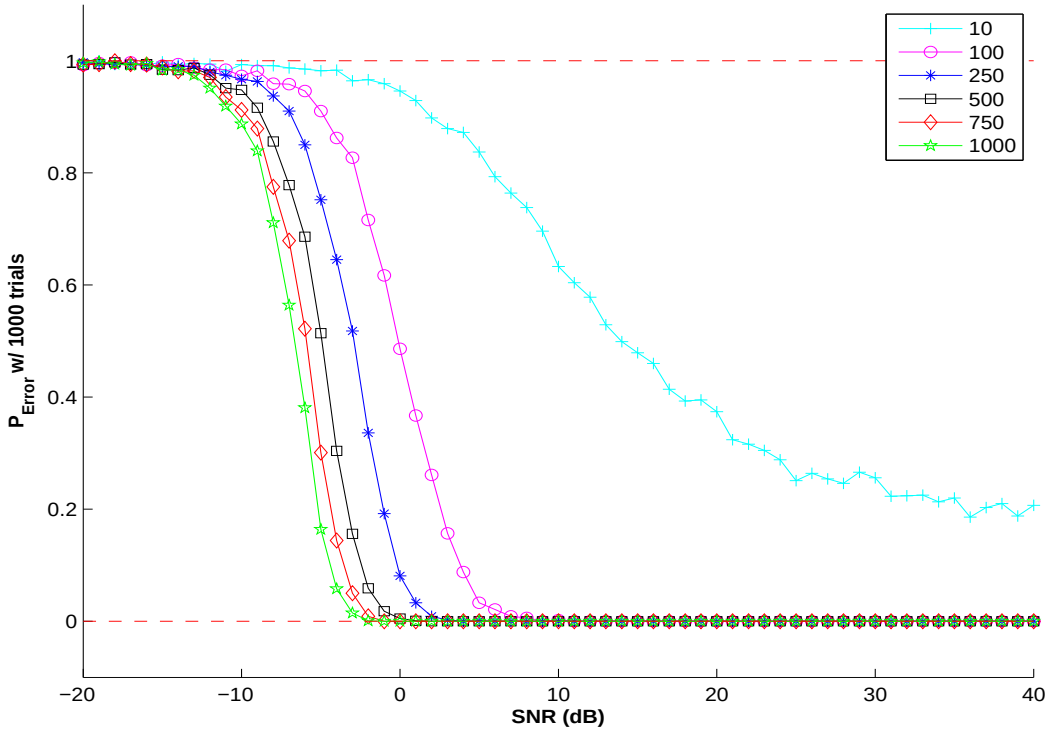

(b) Frequency Domain

Figure 4.7: Feature (AVERAGE SYMBOL PHASE) correlation results averaged over 1000 trials. (a) Time Domain (b) Frequency Domain

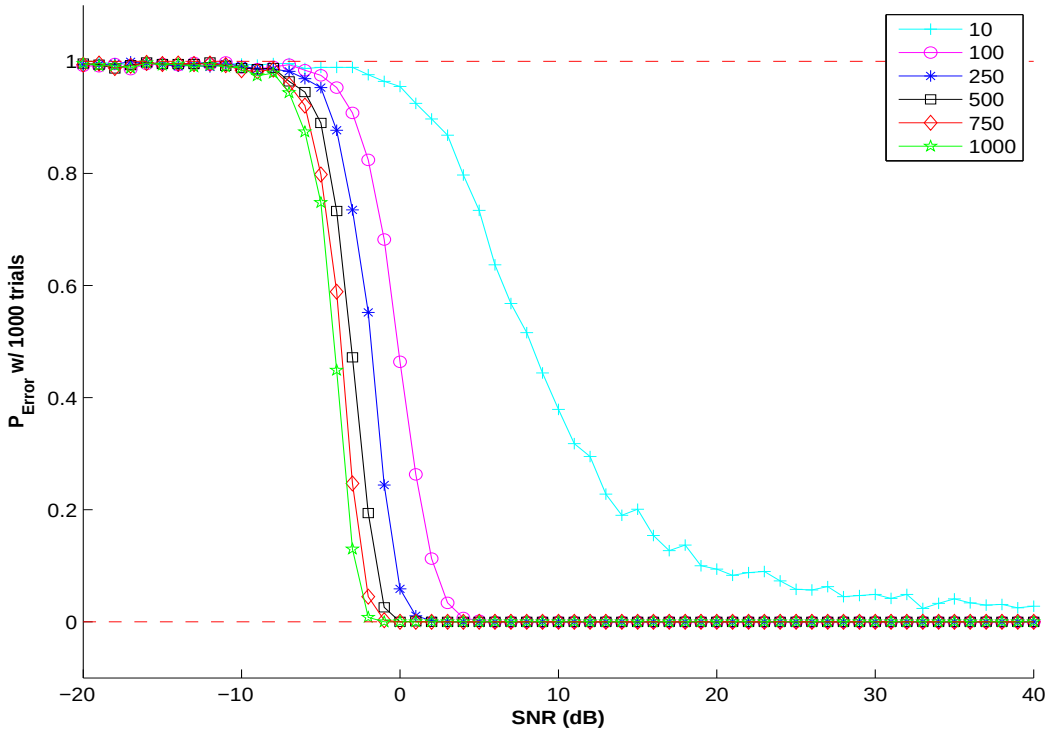

(a) Time Domain

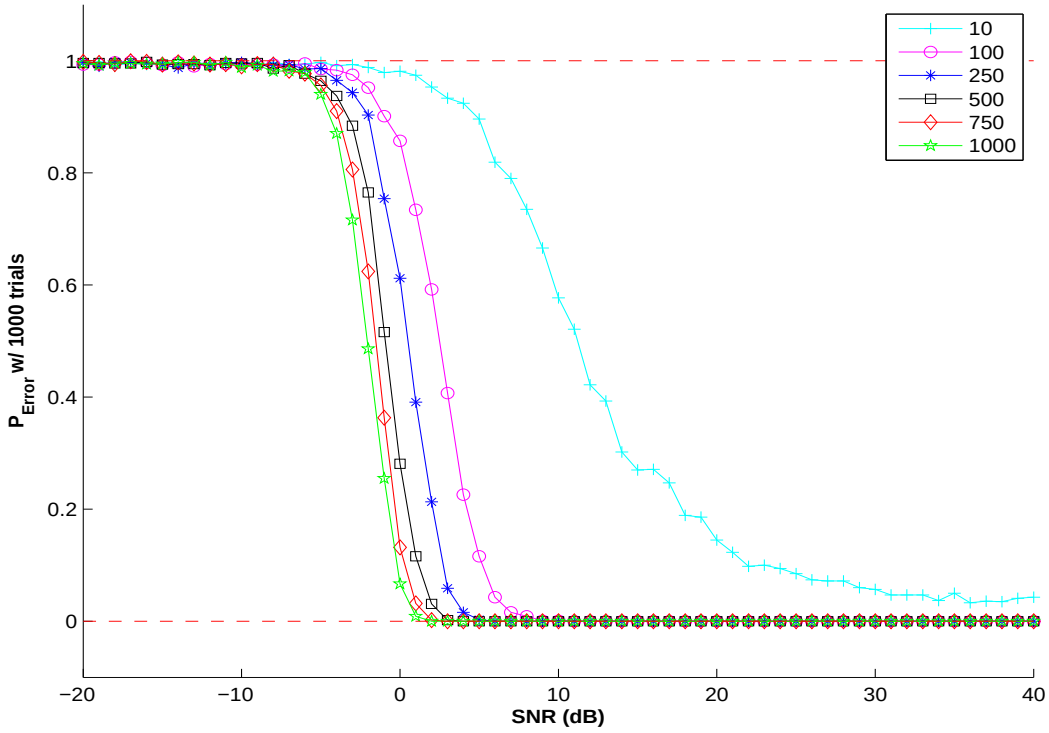

(b) Frequency Domain

Figure 4.8: Feature (RMS) correlation results averaged over 1000 trials. (a) Time Domain (b) Frequency Domain

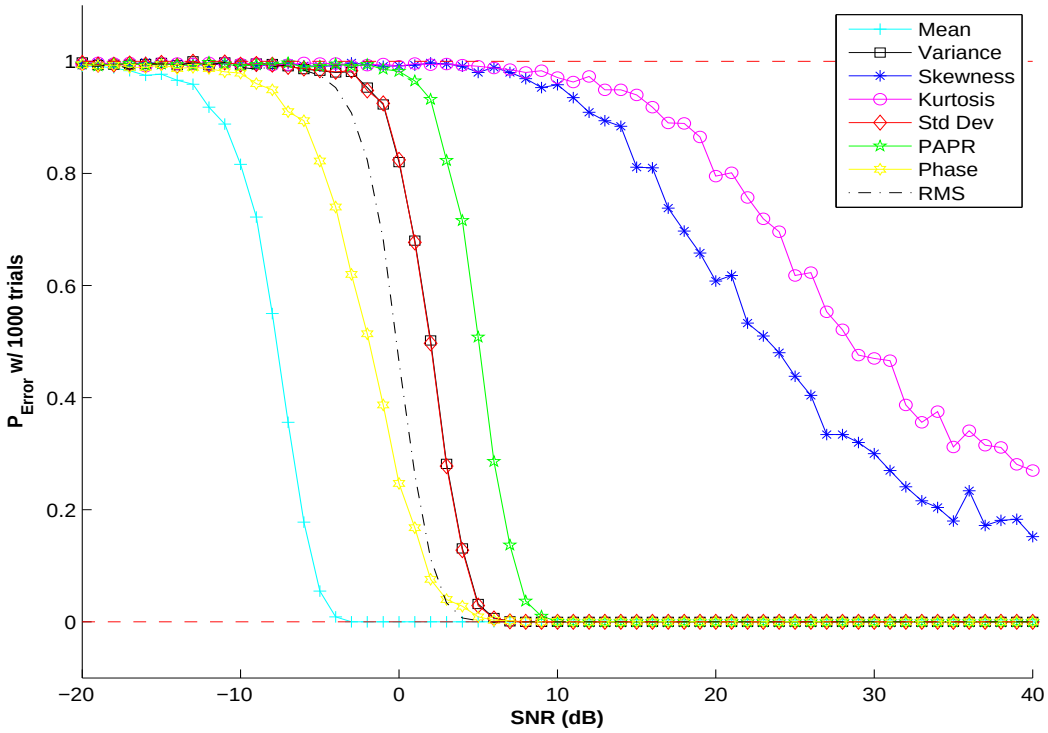

(a) Time Domain

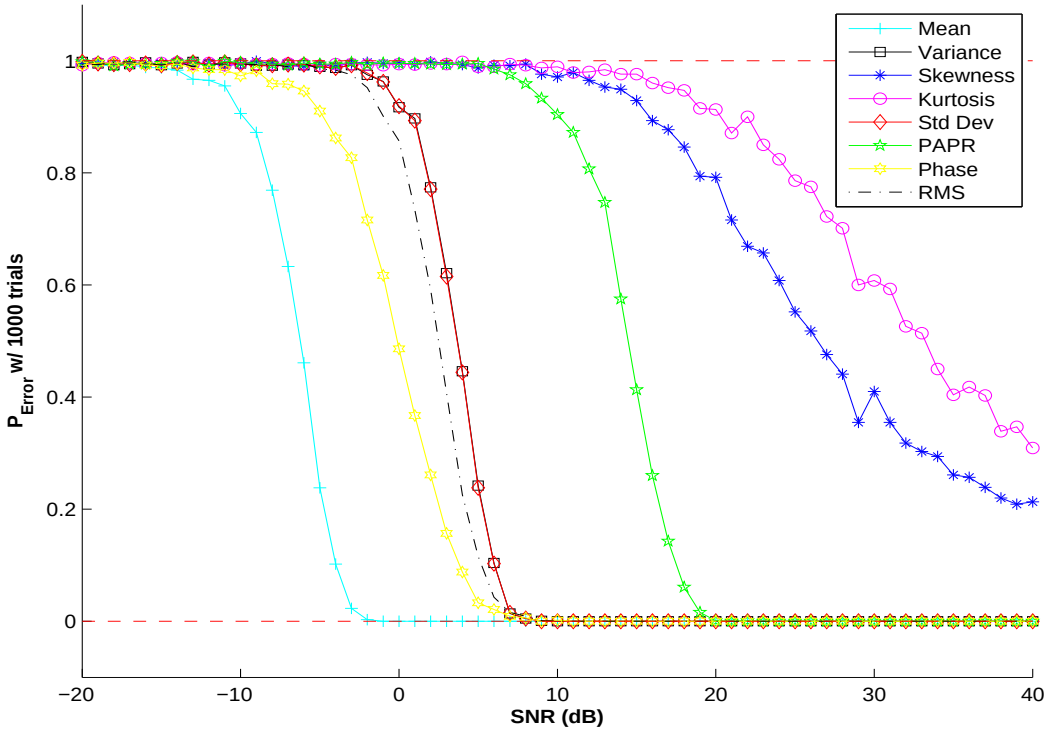

(b) Frequency Domain

Figure 4.9: All Features at a Window Size of 100 symbols averaged over 1000 trials. (a) Time Domain (b) Frequency Domain

V. Conclusions and Recommendations

To rehighlight, the development and characterization of a feature-based correlator for the purposes of calculating TDOA measurements was presented in this document. Chapter I introduced the research motivation, related areas, and goals which guided the research. A technical background detailing typical OFDM structure was given in Chapter II, while Chapter III provided the specific framework and specifications for the proof-of-concept model. Finally, Chapter IV provided the validation, modeling and simulation results for the feature correlator. This chapter first summarizes the key findings from Chapter IV and offers several research directions which may be taken to further develop this proof-of-concept.

5.1 Conclusion

Performance of the proposed feature-based symbol correlation process depends on the three variables listed below. Several insights can be drawn on how each of these variables affect the overall performance. The three variables are as follows:

1. The *window size* over which the symbol features are correlated directly affect the symbol shift estimation. From the results in Chapter IV, a *window size* of 100 or greater should be used to achieve the highest accuracy for given SNR value.
2. The channel noise level affects the signal in such a way that all features become unusable for TDOA calculations at their respect "low" SNR values. As expected, the symbol feature correlator accuracy increases as the SNR increases.
3. The total symbol size also affects feature correlator accuracy. Comparing the correlator's frequency and time domain plots in Chapter IV illustrates this point. Remember that in the frequency domain the correlator symbol size is only N samples whereas in the time domain the symbol size is $M = N + \nu$.

This feature-based correlation proof-of-concept exploits the inherent signal structure of the OFDM signals, which are becoming widely used in wireless systems. As demonstrated, the proposed correlation process is effective in estimating symbol differences between two receivers at SNRs as low as approximately -5 dB when using the mean feature. However, other features such as skewness and kurtosis are not suitable for estimating symbol shifts and ultimately TDOA calculations.

5.2 Recommendations for Future Research

This research focused exclusively on software simulations, but there are many areas of opportunity to expand on this research. A few such areas are listed below.

- **TDOA Measurements**

  Due to time constraints, actual TDOA measurements were never taken. It will be necessary to implement the TDOA algorithm, (3.17), developed in Section 3.2 to determine the exact accuracy and usefulness of navigating with OFDM signals.

- **Different Channel Models**

  The only channel model simulated in this thesis was an AWGN channel. There many different channel models which will make this proof-of-concept more realistic. For example, there is a real need to develop a multipath channel model, since OFDM is design to combat the effects of multipath.

- **Different Sampling Rates**

  For this thesis, the OFDM signal was sampled at exactly the Nyquist rate. It is necessary to understand the possible effects of over- and undersampling of the feature correlator and TDOA calculations.

- **Real-World Experimentation**

  Since this research focused solely on software simulations, hardware implementation and experimentation would be an essential next step. It would be possible

to use simple 802.11a/g/n routers as a transmission source. Also, it may be possible to collect satellite radio terrestrial repeater signals.

- **More Features**

  Only eight statistical features were chosen for this research, but it definitely is imperative to experiment with other features to determine whether or not they could be potential candidates for the proposed feature-based correlator.

This research has proven in a simulation proof-of-concept environment that an OFDM feature-based correlator could be used for symbol difference estimation and ultimately reliable, accurate TDOA calculations.

Appendix A. OFDM Signal Generator

This appendix contains the Matlab® code used for all the research simulations.

Listing A.1: Main Program (OFDM_main.m)

```
%-------------------------------------------------------------
%                  Transmitted Signal Settings
%-------------------------------------------------------------

CP_length = 16; % Length of Cyclic Prefix
data_length = 64; % Length of Data
num_of_symbols = 2048; % Number of Transmitted Symbols
                       % Recommend ≥ 20

pilot_freq_correlation = 0; % Do pilot freq corr?
                            % (1 == yes, 0 == no)
pilot_freqs_per_symbol = 0; % Number of Pilot Freq per Symbol
pilot_freq_repeat = 0; % Symbol number when the pilots freqs will ...
   repeat in transmitted signal (NOTE:  Must ≥ (data_length + ...
   CP_length)/2 + 1)

plot_features = 1; % Plot feature correlations?  (1 == yes, 0 == ...
   no) (NOTE: make sure trials are low for you will get feature ...
   plots for EACH trial)
plot_error = 0; % Plot error for each feature?  (1 == yes, 0 == no...
   )
window_size = 100;  % Select rcvr_1_feature window size (See ...
   rcvr_1_window ¬ line 152 in test.m)

% Select transmission modulation type (power of 2)
    % M = 4 (4-QAM), M = 16 (16-QAM), M = 64 (64-QAM)
M = 64;

% Select number of trials to run per feature per domain
trials = 1;

symbol_length = CP_length + data_length; % Entire Symbol Length

%-------------------------------------------------------------
%                     Noise Signal Settings
%-------------------------------------------------------------

%----------------- Receiver # 1:  Fixed Receiver -----------

noise_rcvr_1 = 0;  % Add AWGN to output signal
                   %   (1 == Add noise; 0 == No Noise)

% SNR_rcvr_1 = -10:5:15;
SNR_rcvr_1 = 5;  % SNR out of transmitter in dB (used to determine...
    noise)
```

```
40
   %----------------- Receiver # 2:  Mobile Receiver ----------

   noise_rcvr_2 = 1;  % Add AWGN to output signal
                      % (1 == Add noise; 0 == No Noise)
45 SNR_rcvr_2 = SNR_rcvr_1;   % SNR out of transmitter in dB (used to...
       determine noise)

   %-------------------------------------------------------------
   %                            Sync Signal
   %-------------------------------------------------------------
50
   %----------------- Receiver # 1:  Fixed Receiver -----------

   % Synchronous or Asynchronous signal (1 == Async, 0 == Sync)
   sync_rcvr_1 = 1;
55
   max_shift_rcvr_1 = 100;   % Specify the maximum number of symbols ...
      to shift (i.e. max_shift = 1 means shift will be between 1 & ...
      num_of_symbols)

   %----------------- Receiver # 2:  Mobile Receiver ----------

60 sync_rcvr_2 = 1;   % Synchronous or Asynchronous signal (1 == ...
      Async, 0 == Sync)
   max_shift_rcvr_2 = max_shift_rcvr_1;  % Specify max no. of symbols...
       to shift (i.e. max_shift = 1 means shift will be between 1 & ...
      num_of_symbols)

   %-------------------------------------------------------------
   %              Initialize trials w/ different SNR values
65 %-------------------------------------------------------------

   % Preallocate memory for speed
   actual_symbol_shift = zeros(length(SNR_rcvr_1), trials);
   error_freq = zeros(length(SNR_rcvr_1), trials, 8); % 8 = no. of ...
      features
70 error_time = zeros(length(SNR_rcvr_1), trials, 8); % 8 = no. of ...
      features

   for snr = 1:length(SNR_rcvr_1)
       for trls = 1:trials

75 %-------------------------------------------------------------
   %                     Generate OFDM signal (w/ no noise)
   %-------------------------------------------------------------

           % Used for debugging OFDM_generator.m function
80         % dbstop in OFDM_generator.m at 40
```

```
        [rcvd_signal_no_noise, pilot_freqs, pilot_freq_matrix] = ...
           OFDM_generator(CP_length, data_length, num_of_symbols, ...
           M, pilot_freqs_per_symbol, pilot_freq_repeat);

%-------------------------------------------------------------
%                    Receiver # 1:  Fixed Receiver
%-------------------------------------------------------------

        [rcvr_1_signal, rcvr_1_signal_features_time, ...
           rcvr_1_signal_features_freq, rcvr_1_shift, rcvr_1_delta, ...
           R_1_pilot, R1_bound, R1_bound_avg] = OFDM_receiver(...
           rcvd_signal_no_noise, noise_rcvr_1, SNR_rcvr_1(snr), ...
           sync_rcvr_1, max_shift_rcvr_1, symbol_length, CP_length...
           , data_length, pilot_freq_matrix, ...
           pilot_freq_correlation);

%-------------------------------------------------------------
%                    Receiver # 2:  Mobile Receiver
%-------------------------------------------------------------

        [rcvr_2_signal, rcvr_2_signal_features_time, ...
           rcvr_2_signal_features_freq, rcvr_2_shift, rcvr_2_delta, ...
           R_2_pilot, R2_bound, R2_bound_avg] = OFDM_receiver(...
           rcvd_signal_no_noise, noise_rcvr_2, SNR_rcvr_2(snr), ...
           sync_rcvr_2, max_shift_rcvr_2, symbol_length, CP_length...
           , data_length, pilot_freq_matrix, ...
           pilot_freq_correlation);

%-------------------------------------------------------------
%     Calculate Actual Generated Symbol Shift Btwn Rcvrs
%-------------------------------------------------------------

        actual_symbol_shift(snr,trls) = floor(rcvr_2_shift/...
           symbol_length) - floor(rcvr_1_shift/symbol_length);

%-------------------------------------------------------------
%            Receiver Correlation:  Determine Symbol Locations
%-------------------------------------------------------------

        % Used for debugging OFDM_feature_correlator.m function
        % dbstop in OFDM_feature_correlator.m at 9

        % Preallocate Memory for Speed
        R_features_time = zeros(8, max_shift_rcvr_1 + 1, length(...
           window_size));
        R_features_freq = zeros(8, max_shift_rcvr_1 + 1, length(...
           window_size));
        R_time_index = zeros(8,1, length(window_size));
        R_freq_index = zeros(8,1, length(window_size));
```

```
115         % Correlate symbol featutues in both time and freq domains
            % i = feature (i.e. 1 == mean, 2 == variance, etc.)

            % dbstop in OFDM_feature_correlator.m at 37
            % dbstop in OFDM_feature_correlator.m at 75
120         for i = 1:size(rcvr_1_signal_features_time,2)
                for win_sz = 1:length(window_size)

                % How many Symbol features would you like to compare w...
                   / rcvr 1 ?
                % (NOTE: Max/Min Window Bounds:
125             %    Min Lower bound > 2 + max_shift_rcvr_1
                %   Max Upper bound < 2 + max_shift_rcvr_1 -
                %                       length(rcvr_1_signal_features)
                % buffer U/L bounds by + 2 in order to filter
                    rcvr_1_window = [256 (256 + window_size(win_sz))];
130
                    [R_ftrs_time R_ftrs_freq] = OFDM_feature_correlator...
                       (rcvr_1_signal_features_time(rcvr_1_window(1):rcvr_1_window...
                       (2),i), rcvr_2_signal_features_time(rcvr_1_window...
                       (1) - max_shift_rcvr_1 - 2:rcvr_1_window(2) + max_shift_rcvr_1
                        + 2,i), rcvr_1_signal_features_freq(rcvr_1_window...
                       (1):rcvr_1_window(2),i), rcvr_2_signal_features_freq...
                       (rcvr_1_window(1) - max_shift_rcvr_1 -  2:rcvr_1_window...
                       (2) + max_shift_rcvr_1 + 2,i),...
                        i, rcvr_1_window);

                    % Do this to so we can place different sized ...
                       vectors into
135                 %   one matrix
                    R_features_time(i,1:length(R_ftrs_time), win_sz)...
                        = R_ftrs_time;
                    R_features_freq(i,1:length(R_ftrs_freq), win_sz)...
                        = R_ftrs_freq;

                    % Calculate symbol shift (i.e. R_????_index)
140                 [c R_time_index(i,:,win_sz)] = max(R_features_time...
                       (i,:, win_sz));
                    [c R_freq_index(i,:,win_sz)] = max(R_features_freq...
                       (i,:, win_sz));
                    clear c;

                    % Adjust index
145                 R_time_index(i,:, win_sz) = R_time_index(i,:, ...
                       win_sz) - max_shift_rcvr_1 - 1;
                    R_freq_index(i,:, win_sz) = R_freq_index(i,:, ...
                       win_sz) - max_shift_rcvr_1 - 1;

                    % Plot Correlation results
                    if plot_features == 1
```

```
                    [x] = OFDM_plot_features(i, max_shift_rcvr_1, ...
                        R_features_time, R_features_freq, ...
                        noise_rcvr_1, SNR_rcvr_1); clear x;
                end

            % Calculate the number of errors
            % *** error_????(SNR, Trial, Feature, Window Size)
            % rows = SNR
            % columns = Trials
            % 3rd-dimension = Feature
            % 4th-dimension = Window Size
                if actual_symbol_shift(snr,trls) - R_freq_index(i...
                    ,:,win_sz) == 0
                    error_freq(snr,trls,i,win_sz) = 0;
                else
                    error_freq(snr,trls,i,win_sz) = 1;
                end

                if actual_symbol_shift(snr,trls) - R_time_index(i...
                    ,:,win_sz) == 0
                    error_time(snr,trls,i,win_sz) = 0;
                else
                    error_time(snr,trls,i,win_sz) = 1;
                end
            end
        end
    end
end; clear snr trls i

if plot_error == 1

    % Preallocate memory for speed
    error_time_mean = zeros(8,length(SNR_rcvr_1),length(...
        window_size));
    error_freq_mean = zeros(8,length(SNR_rcvr_1),length(...
        window_size));

    % Calculate Probabilty of Error
    for win_sz = 1:length(window_size)
        for i = 1:8
            for snr = 1:length(SNR_rcvr_1)
                error_time_mean(i,snr,win_sz) = mean(error_time(...
                    snr,:,i,win_sz));
                error_freq_mean(i,snr,win_sz) = mean(error_freq(...
                    snr,:,i,win_sz));
            end
        end
    end
end; clear snr trls i
```

Listing A.2: OFDM Generator Function (OFDM_generator.m)

```
function [rcvd_signal, pilot_freqs, pilot_freq_matrix] = ...
    OFDM_generator(CP_length, data_length, num_of_symbols, M, ...
    pilot_freqs_per_symbol, pilot_freq_repeat)

% Calculate Spacing between pilot freqs on a per symbol basis
spacing_btwn_pilot_freqs = floor(data_length/...
    pilot_freqs_per_symbol);

% Calculate Entire Symbol Length
symbol_length = CP_length + data_length;

% Determines range of values (used for QAM)
alphabet = ((-(sqrt(M)-1)):2:(sqrt(M)-1))' * ones(1,sqrt(M)) + j...
    * ones(sqrt(M),1) * ((-(sqrt(M)-1)):2:(sqrt(M)-1));

% Generate Random QAM Sequence for Pilot Frequencies
pilot_freqs = randsrc(pilot_freq_repeat, pilot_freqs_per_symbol, ...
    reshape(alphabet, 1, M));

% Generate QAM-mapped transmitted signal
if M == 4 || M == 16 || M == 64
    x = randsrc(1,(num_of_symbols * data_length), reshape(alphabet...
        , 1, M));
end

% x = ones(1,(num_of_symbols * data_length));

% Normalize
pwr = (sqrt(mean(x.^2)));
x = x./ pwr;
pilot_freqs = pilot_freqs./pwr;

% Divide Generated signal into symbols
x_symbols = (reshape(x, data_length , num_of_symbols)).';

% Preallocate memory for speed
pilot_freq_matrix = zeros(num_of_symbols, data_length);
x_ifft = zeros(num_of_symbols, data_length);
cp = zeros(num_of_symbols, CP_length);
x_received = zeros(num_of_symbols, symbol_length);

for i = 1:1:num_of_symbols

    % Insert Pilot Freqs according to parameters ...
       pilot_freqs_per_symbol and pilot_freq_repeat
    if mod(i,pilot_freq_repeat) == 0;
        k = pilot_freq_repeat;
    else
```

```
            k = mod(i,pilot_freq_repeat);
        end

        for m = 1:1:pilot_freqs_per_symbol
            if mod(k + (m-1)* spacing_btwn_pilot_freqs, data_length)...
                == 0
                x_symbols(i,data_length)= pilot_freqs(k,m);
                pilot_freq_matrix(i,data_length) = pilot_freqs(k,m);
            else
                x_symbols(i,mod(k+(m-1)* spacing_btwn_pilot_freqs, ...
                    data_length)) = pilot_freqs(k,m);
                pilot_freq_matrix(i,mod(k+(m-1)*...
                    spacing_btwn_pilot_freqs, data_length)) = ...
                    pilot_freqs(k,m);
            end
        end

        % Take the ifft of each symbol
        x_ifft(i,:) = ifft(x_symbols(i,:));

        % Calculate the Cyclic Prefix
        cp(i,:) = x_ifft(i, (data_length + 1 - CP_length) : ...
            data_length);

        % Append the CP to the correct symbols
        x_received(i,:) = [cp(i,:) x_ifft(i,:)];

    end; clear i m k;

    pilot_freq_matrix = pilot_freq_matrix(1:pilot_freq_repeat, 1:...
        data_length);

    % Turn x_received matrix into a vector
    rcvd_signal = reshape(x_received.', 1, []);

    return
```

Listing A.3: OFDM Receiver Function (OFDM_receiver.m)

```
function [rcvd_signal, rcvd_signal_features_time, ...
    rcvd_signal_features_freq, shift, Δ, R_symbol, R, R_avg] = ...
    OFDM_receiver(rcvd_signal_no_noise, noise, SNR, sync, max_shift...
    , symbol_length, CP_length, data_length, pilot_freq_matrix, ...
    pilot_freq_correlation)

%-----------------------------------------------------
% Add AWGN to Transmitted Signal...if Desired (Change Setting in ...
    Main file)
%-----------------------------------------------------

if noise == 1
    rcvd_signal = awgn(rcvd_signal_no_noise, SNR, 'measured');
else
    rcvd_signal = rcvd_signal_no_noise;
end

%-----------------------------------------------------
%       Make Asynchronous...if Desired (Change Setting in Main ...
    file)
%-----------------------------------------------------

if sync == 1
    shift = randint(1,1,[1 (max_shift * (symbol_length-1))]);
    rcvd_signal = circshift(rcvd_signal, [0 shift]);
else
    shift = 0;
end

%=====================================================
%                     OFDM RECEIVER
%=====================================================

%-----------------------------------------------------------
%     Correlation Algorithm (reference: van de Beek)
%-----------------------------------------------------------

% Preallocate memory for speed
R = zeros(1,length(rcvd_signal) - (symbol_length));

for m = 0:1:length(rcvd_signal) - (symbol_length)
    R(m+1) = (rcvd_signal(m + ((data_length+1):(symbol_length))))...
        * (conj(rcvd_signal(m + (1:CP_length)))).';
end; clear m;

R = real(R);
```

```
% Average the peaks to determine a better estimate of correlation ...
    maximums

% Determine the number of symbols to average over
sym_no = 1;

% Preallocate for speed
R_avg = zeros(1,(sym_no * (symbol_length)));

% Average over sym_no of symbols
for i = 1:1:floor(length(R)/(sym_no * (symbol_length)))
    R_avg = R_avg + R((1 + (i - 1) * sym_no * (symbol_length)):(i...
        * sym_no * (symbol_length)));
end; clear i;

% Calculate max shift
[c ∆] = max(R_avg(1:(symbol_length))); clear c;

rcvd_signal = rcvd_signal(∆:end);
rcvd_signal = rcvd_signal(1:floor(length(rcvd_signal)/...
    symbol_length)*symbol_length);

%-------------------------------------------------------
%          Calculate Symbol Features in Time Domain
%-------------------------------------------------------

%------------------- Divide rcvd_signal into symbols --

% Reshape rcvd_signal so that each symbol corresponds to a row in ...
    matrix
rcvd_signal_symbols = (reshape(rcvd_signal, [], floor(length(...
    rcvd_signal)/symbol_length))).';

% Preallocate for speed
rcvd_signal_features_time = zeros(size(rcvd_signal_symbols,1),8);

for i = 1:1:size(rcvd_signal_symbols,1)

%------------ Column 1:  Symbol Mean --------------------
    rcvd_signal_features_time(i,1) = mean(rcvd_signal_symbols(i,:)...
        ,2);

%------------ Column 2:  Symbol Variance ----------------
    rcvd_signal_features_time(i,2) = var(rcvd_signal_symbols(i,:)...
        ',1);

%------------ Column 3:  Symbol Skewness ----------------
    rcvd_signal_features_time(i,3) = skewness(rcvd_signal_symbols(...
        i,:)',0);
```

```
    %------------ Column 4:  Symbol Kurtosis ----------------
85      rcvd_signal_features_time(i,4) = kurtosis(rcvd_signal_symbols(...
            i,:)');

    %------------ Column 5:  Symbol Standard Deviation ------
        rcvd_signal_features_time(i,5) = std(rcvd_signal_symbols(i,:)...
            ',1);

90  %--- Column 6:  Symbol Peak - to - Average Power Ratio ---
        rcvd_signal_features_time(i,6) = max(abs(rcvd_signal_symbols(i...
            ,:)).^2) / mean(abs(rcvd_signal_symbols(i,:)).^2);

    %------------ Column 7:  Symbol Average Phase ------------
        rcvd_signal_features_time(i,7) = atan2(mean(imag(...
            rcvd_signal_symbols(i,:))), mean(real(rcvd_signal_symbols(i...
            ,:))));
95
    %------------ Column 8:  Symbol Root-Mean Square (RMS) ---
        rcvd_signal_features_time(i,8) = sqrt(mean(rcvd_signal_symbols...
            (i,:).^2));

    end; clear i;
100
    %-------------------------------------------------------------
    %          Remove Cyclic Prefix from Rcvd Signal and FFT
    %-------------------------------------------------------------

105 % Remove Cyclic Prefix
    rcvd_signal_no_CP = rcvd_signal_symbols(:,CP_length + 1:end);

    % FFT Received Signal
    rcvd_signal_fft = (fft(rcvd_signal_no_CP.')).';
110
    %-------------------------------------------------------------
    %                Calculate Symbol Features in Freq Domain
    %-------------------------------------------------------------

115 % Preallocate for speed
    rcvd_signal_features_freq = zeros(size(rcvd_signal_fft,1),8);

    for i = 1:1:size(rcvd_signal_fft,1)

120 %------------ Column 1:  Symbol Mean --------------------------
        rcvd_signal_features_freq(i,1) = mean(rcvd_signal_fft(i,:),2);

    %------------ Column 2:  Symbol Variance ----------------------
        rcvd_signal_features_freq(i,2) = var(rcvd_signal_fft(i,:)',1);
125
    %------------ Column 3:  Symbol Skewness ----------------------
```

```
        rcvd_signal_features_freq(i,3) = skewness(rcvd_signal_fft(i,:)...
            ');

    %------------ Column 4:  Symbol Kurtosis ----------------------
130     rcvd_signal_features_freq(i,4) = kurtosis(rcvd_signal_fft(i,:)...
            ');

    %------------ Column 5:  Symbol Standard Deviation ------------
        rcvd_signal_features_freq(i,5) = std(rcvd_signal_fft(i,:)',1);

135 %------- Column 6:  Symbol Peak - to - Average Power Ratio ----
        rcvd_signal_features_freq(i,6) = max(abs(rcvd_signal_fft(i,:))...
            .^2) / mean(abs(rcvd_signal_fft(i,:)).^2);

    %------------ Column 7:  Symbol Average Phase -----------------
        rcvd_signal_features_freq(i,7) = atan2(mean(imag(...
            rcvd_signal_fft(i,:))), mean(real(rcvd_signal_fft(i,:))));
140
    %------------ Column 8:  Symbol Root-Mean Square (RMS) --------
        rcvd_signal_features_freq(i,8) = sqrt(mean(rcvd_signal_fft(i...
            ,:).^2));

    end; clear i;
145
    %-------------------------------------------------------------
    %               Correlate Received Signal w/ Pilot Freqs
    %                   to Determine Total Symbol Shift
    %-------------------------------------------------------------
150
    if pilot_freq_correlation == 1

        % Preallocate memory for speed
        R_symbol = zeros((size(pilot_freq_matrix, 1)*2) -1, 1);
155
        % Correlate Pilot Freqs w/ Rcvd Signal
        for m = 0:1:size(pilot_freq_matrix, 1)-1
            R_symbol(m+1) = sum(sum((pilot_freq_matrix. * conj(...
                rcvd_signal_fft((m+1:(m + size(pilot_freq_matrix, 1)))...
                ,:)))));
        end; clear m;
160
    % Calculate index where max value occurs (this minus 1 equals ...
       total
      % number of symbols the received signal is shifted by)

        [c sym_shift] = max(R_symbol);
165
        R_symbol = real(R_symbol);

    %-------------------------------------------------------------
```

```
%                                   Plot Results
%-------------------------------------------------------------------

    figure()
    subplot(2,1,1)
    plot(0:(data_length+CP_length-1), R_symbol(1:(data_length+...
        CP_length)));
    xlabel('Symbol Index (i.e. Total Symbol Shift)', 'fontweight',...
        'bold','fontsize',18);

    if noise == 1
        title({['Frequency Correlation with SNR = ', num2str(SNR),...
            ' dB']},'fontweight','bold','fontsize',18);
    else
        title('Frequency Correlation with No Noise', 'fontweight',...
            'bold','fontsize',18);
    end

    text(sym_shift-1,c,{['  \leftarrow Total Symbol Shift = ', ...
        num2str(sym_shift-1)]}, 'HorizontalAlignment','left',...
        'fontweight','bold','fontsize',14);

    subplot(2,1,2)
    plot(0:(length(R_avg)-1), R_avg/floor(length(R)/(sym_no * ...
        symbol_length)))
    title({['Time Correlation Averaged Across ', num2str(sym_no),'...
        Peak(s)']},'fontweight','bold','fontsize',18);
    xlabel('Total Shift within Symbol','fontweight','bold','...
        fontsize',18);

    [c i] = max(R_avg/floor(length(R)/ (sym_no * symbol_length)));
    text(i-1,c,{['  \leftarrow Total Shift w/in Symbol = ', ...
        num2str(i-1)]}, 'HorizontalAlignment','left', 'fontweight',...
        'bold','fontsize',14);

else
    % Bogus variable...used to make function work
    R_symbol = zeros((size(pilot_freq_matrix, 1)*2) -1, 1);
end
```

Listing A.4: OFDM Symbol Feature Correlator (OFDM_feature_correlator.m)

```
function [R_features_time, R_features_freq] = ...
    OFDM_feature_correlator(rcvr_1_signal_features_time, ...
    rcvr_2_signal_features_time, rcvr_1_signal_features_freq, ...
    rcvr_2_signal_features_freq, count, window)

% Preallocate Memory for Speed
R_features_time = zeros(1,length(rcvr_2_signal_features_time) - ...
    length(rcvr_1_signal_features_time) + 1);

% Correlate Symbol Features in Time Domain
for m = 0:1:length(rcvr_2_signal_features_time) - length(...
    rcvr_1_signal_features_time) - 4

    A = rcvr_1_signal_features_time(1:length(...
        rcvr_1_signal_features_time));
    B = rcvr_2_signal_features_time((m + 1:(m + length(...
        rcvr_1_signal_features_time))));

    R_features_time(m+1) = (A - mean(A)).'*conj((B - mean(B)));

end; clear m;

% Preallocate Memory for Speed
R_features_freq = zeros(1,length(rcvr_2_signal_features_freq) - ...
    length(rcvr_1_signal_features_freq) + 1);

% Correlate Symbol Features in Freq Domain
for m = 0:1:length(rcvr_2_signal_features_freq) - length(...
    rcvr_1_signal_features_freq) - 4

    A = rcvr_1_signal_features_freq(1:length(...
        rcvr_1_signal_features_freq));
    B = rcvr_2_signal_features_freq((m+1:(m + length(...
        rcvr_1_signal_features_freq))));

    R_features_freq(m+1) = (A - mean(A)).'*conj((B - mean(B)));

end; clear m;

% Filter results to get "cleaner" results
if count == 2 || count == 5 || count == 6 || count == 8
    R_features_time = conv(abs(R_features_time), [-1 2 -1]);
    R_features_freq = conv(abs(R_features_freq), [-1 2 -1]);
    R_features_time = R_features_time(4:end-3);
    R_features_freq = R_features_freq(4:end-3);
else
    R_features_time = abs(R_features_time(3:end-2));
    R_features_freq = abs(R_features_freq(3:end-2));
```

```
    end
40  return;
```

Bibliography

1. Chairman, Joint Chiefs of Staff. US Department of Defense. Joint Vision 2010. [Online]. Available at http://www.dtic.mil/. [Accessed 15-June-2007].

2. Institute of Electrical and Electronics Engineers. New York, NY. *IEEE Std 802.15.3^{TM}-2003, IEEE Standard for Information technology-Telecommunication and information exchange between systems-Local and metropolitan area networks-Specific requirements , Part 15.3: Wireless Medium Access Control (MAC) and Physical Layer (PHY) Specifications for High Rate Wireless Personal Area Networks (WPANs)*. 2003.

3. Institute of Electrical and Electronics Engineers. Piscataway, NJ. *IEEE Std 802.11a-1999(R2003), IEEE Standard for Information technology-Telecommunication and information exchange between systems-Local and metropolitan area networks-Specific requirements, Part 11: Wireless LAN Medium Access Control (MAC) and Physical Layer (PHY) Specifications: High-speed Physical layer in the 5 GHz Band*. 1999, Revised 2003.

4. Institute of Electrical and Electronics Engineers. New York, NY. *IEEE Std 802.16^{TM}-2004, IEEE Standard for Local and Metropolitan Area Networks, Part 16: Air Interface for Fixed Broadband Wireless Access Systems*. 2001, Revised 2004.

5. European Telecommunications Standards Institute, "Digital Video Broadcasting (DVB): Implementation guidelines for DVB terrestrial services; transmission aspects," European Telecommunications Standards Institute, ETSI TR-101-190, 1997. [Online]. Available at http://www.etsi.org. [Accessed: July 3, 2007].

6. Bahai, Ahmad, Burton Saltzberg and Mustafa Ergen. *Multi-Carrier Digital Communications Theory and Applications of OFDM*. Springer Science+Business Media, Inc., New York, NY, second edition, 2004.

7. Bucher, Mary. "Simulation of Multipath Fading/Ghosting for Analog and Digital Television Transmission in Broadcast Channels". *IEEE Transactions on Broadcasting*, 38(4):256–262, December 1992.

8. Burr, A.G. "The Multipath Problem: An Overview". *IEE Colloquium on Multipath Countermeasures*. Institution of Electrical Engineers (IEE), London, UK, May 1996.

9. Caffery, James J., Jr. and Gordon L. Stüber. "Overview of Radiolocation in CDMA Cellular Systems". *IEEE Communications Magazine*, 36(4):38–45, April 1998.

10. Dowla, Farid (editor). *Handbook of RF and Wireless Technologies*. Elsevier, Inc., Burlington, MA, 2004.

11. Eggert, Ryan J. *Evaluating the Navigation Potential of the National Television System Committe Broadcast Signal*. Master's thesis, Graduate School of Engineering, Air Force Institute of Technology (AETC), Wright-Patterson AFB OH, March 2004. AFIT/GE/ENG/04-08.

12. Henkel, Werner, Georg Tauböck, Per Ödling, Per Ola Börjesson, and Niklas Petersson. "The Cyclic Prefix of OFDM/DMT - An Analysis". *2002 International Zurich Seminar on Broadband Communications. Access, Transmission, Networking.*, 22.1 – 22.3. Institute of Electrical and Electronics Engineers (IEEE), Zurich, Switzerland, February 2002.

13. Jiang, Yingtao, Ting Zhou, Yiyan Tang, and Yuke Wang. "Twiddle-Factor-Based FFT Algorithm with Reduced Memory Access". *Proceedings of the Intrnational Parallel and Distributed Processing Symposium*, 70–77. Institute of Electrical and Electronics Engineers (IEEE), IEEE Computer Society, Ft. Lauderdale, FL, April 2002.

14. Kim, Bryan S. *Evaluating the Correlation Characteristics of Arbitrary AM and FM Radio Signals for the Purpose of Navigation*. Master's thesis, Graduate School of Engineering, Air Force Institute of Technology (AETC), Wright-Patterson AFB OH, March 2006. AFIT/GE/ENG/06-08.

15. Lin, Shu and Daniel Costello. *Error Control Coding: Fundamental and Applications*. Prentice Hall, Upper Saddle River, NJ, 1983.

16. Ma, Xiaoqiang, Hisashi Kobayashi, and Stuart Schwartz. "Effect of Frequency Offset on BER of OFDM and Single Carrier Systems". *The 14th IEEE International Symposium on Personal, Indoor and Mobile Radio Communication Proceedings*, volume 3, 2239–2243. Institute of Electrical and Electronics Engineers (IEEE), Beijing, China, September 2003.

17. McEllroy, Jonathan A. *Navigation Using Signals of Opportunity in the AM Transmission Band*. Master's thesis, Graduate School of Engineering, Air Force Institute of Technology (AETC), Wright-Patterson AFB OH, September 2006. AFIT/GE/ENG/06-04.

18. Misra, Pratap and Per Enge. *Global Positioning System: Signals, Measurements, and Performance*. Ganga-Jamuna Press, Lincoln, MA, second edition, 2006.

19. van Nee, Richard and Ramjee Prasad. *OFDM for Wireless Multimedia Communications*. Artech House Publishers, Boston, MA, 2000.

20. Santhananthan, K. and C. Tellambura. "Probability of Error Calculation of OFDM Systems with Frequency Offset". *IEEE Communications Magazine*, 49(11):1884–1888, November 2001.

21. van de Beek, Jan-Jaap, Magnus Sandell, and Per Ola Börjesson. "ML Estimation of Time and Frequency Offset in OFDM Systems". *IEEE Transactions on Signal Processing*, 45(7):1800–1805, July 1997.

22. Wikipedia. "Orthogonal Frequency-Division Multiplexing — Wikipedia, The Free Encyclopedia", 2007. [Online]. Available at http://en.wikipedia.org/wiki/OFDM. [Accessed 22-June-2007].

23. Zhao, Yuping and Sven-Gustav Häggman. "Sensitivity to Doppler Shift and Carrier Frequency Errors in OFDM Systems – The Consequences and Solutions". *IEEE 46th Vehicular Technology Conference. 'Mobile Technology for the Human Race'*. Institute of Electrical and Electronics Engineers (IEEE), London, UK, April 1996.

24. Zou, William and Yiyan Wu. "COFDM: An Overview". *IEEE Transactions on Broadcasting*, 41(1):1–8, March 1995.

REPORT DOCUMENTATION PAGE

Form Approved
OMB No. 0704–0188

1. REPORT DATE *(DD–MM–YYYY)*	2. REPORT TYPE	3. DATES COVERED *(From — To)*
13–09–2007	Master's Thesis	Aug 2006 – Sept 2007

4. TITLE AND SUBTITLE

Navigation Using
Orthogonal Frequency Division Multiplexed
Signals of Opportunity

5a. CONTRACT NUMBER

5b. GRANT NUMBER

5c. PROGRAM ELEMENT NUMBER

6. AUTHOR(S)

Jamie S. Velotta, Captain, USAF

5d. PROJECT NUMBER

5e. TASK NUMBER

5f. WORK UNIT NUMBER

7. PERFORMING ORGANIZATION NAME(S) AND ADDRESS(ES)

Air Force Institute of Technology
Graduate School of Engineering and Management (AFIT/EN)
2950 Hobson Way
WPAFB OH 45433-7765

8. PERFORMING ORGANIZATION REPORT NUMBER

AFIT/GE/ENG/07-31

9. SPONSORING / MONITORING AGENCY NAME(S) AND ADDRESS(ES)

Jacob L. Campbell
AFRL/SNRN, AFMC
2241 Avionics Circle, Bldg 620
Wright-Patterson AFB, OH, 45433-7301
DSN: 785-6127 x4154
jacob.campbell@wpafb.af.mil

10. SPONSOR/MONITOR'S ACRONYM(S)

11. SPONSOR/MONITOR'S REPORT NUMBER(S)

12. DISTRIBUTION / AVAILABILITY STATEMENT

APPROVED FOR PUBLIC RELEASE; DISTRIBUTION UNLIMITED.

13. SUPPLEMENTARY NOTES

14. ABSTRACT

The global positioning system (GPS) provides high-accuracy position measurements anywhere in the world. However, a limitation of this system is that a line of sight to multiple satellites is required; therefore, it is unsuitable to use indoors or in urban canyons. Also, in the presence of radio-frequency interference or jamming, GPS may be unavailable. Alternative methods of navigation and positioning are need to either compliment GPS as a backup or for use in areas unreachable by satellites. This research analyzes a feature-based correlation approach for determining reception differences between two Orthogonal Frequency Division receivers for the purpose of TDOA calculations. Multicarrier signals have a very defined signal structure which allows for non-cooperative symbol detection techniques. Simulations are conducted with different correlation windows sizes, SNR values, and eight different statistical features. Out of the eight features tested the symbol mean and average symbol phase proved to be the most promising because they are able to achieve accurate symbol difference estimations at SNR values below 0 dB.

15. SUBJECT TERMS

Orthogonal Frequency Division Multiplex, Signals of Opportunity, Time Difference of Arrival

16. SECURITY CLASSIFICATION OF:			17. LIMITATION OF ABSTRACT	18. NUMBER OF PAGES	19a. NAME OF RESPONSIBLE PERSON
a. REPORT	b. ABSTRACT	c. THIS PAGE			Richard K. Martin, Civ, USAF (ENG)
U	U	U	UU	86	19b. TELEPHONE NUMBER *(include area code)* (937)255–3636 x4526 rmartin@afit.af.mil